COMSATS University Islamabad
Lahore Campus
Library Information Services

turnitin

TURNITIN Originality Report

Title	Molecular Topological Indices Based Analysis of Thermodynamic Properties of Terbium Dioxide

Author	Amir Hassan , ID. SP20-RMT-025
Submission Date	06-Jan-2022 12:36PM (UTC+0500)
Submitted Class	MS. Math & Stat
Submission ID	1738042558
Word Count	14023
Character Count	57463

Similarity Index	14% (Detailed report send to quarter concerned via email)
Remarks	Report seems OK

Note: Bibliography and quoted materials are excluded as per HEC rules

Report Generated By	Nasira Munеer, Assistant Librarian nmunir@cuilahore.edu.pk
Dated on	January 06, 2022

COMSATS UNIVERSITY ISLAMABAD Library Lahore Campus

Lana
06/01/2022

Molecular Topological Indices Based Analysis of Thermodynamics Properties of Terbium Dioxide

By

Amir Hassan

CIIT/SP20-RMT-025/LHR

MS Thesis

In

Mathematics

COMSATS University Islamabad

Lahore Campus-Pakistan

Fall, 2021

COMSATS University Islamabad

Lahore Campus

Molecular Topological Indices Based Analysis of Thermodynamics Properties of Terbium Dioxide

A Thesis Presented to

COMSATS University Islamabad, Lahore Campus

In partial fulfillment

of the requirement for the degree of

MS (Mathematics)

By

Amir Hassan

CIIT/SP20-RMT-025/LHR

Fall-2021

Molecular Topological Indices Based Analysis of Thermodynamics Properties of Terbium Dioxide

A Post Graduate Thesis submitted to the Department of Mathematics as partial fulfillment of the requirement for the award of Degree of MS (Mathematics)

Name	Registration Number
Amir Hassan	CIIT/SP20-RMT-025/LHR

Supervisor

Dr. Sana Javed
Assistant Professor
Department of Mathematics
COMSATS University Islamabad (CUI) Lahore Campus
07 Jan, 2022

Final Approval

This thesis titled

Molecular Topological Indices Based Analysis of Thermodynamics Properties of Terbium Dioxide

By

Amir Hassan

CIIT/SP20-RMT-025/LHR

Has been approved

For the COMSATS University Islamabad, Lahore

External Examiner: _____

Supervisor: _____

Dr. Sana Javed

COMSATS University Islamabad, Lahore Campus

HOD: _____

Dr. Kashif Ali

COMSATS University Islamabad, Lahore Campus

Declaration

I, Amir Hassan, **CIIT/SP20-RMT-025/LHR** hereby declare that I have produced the work presented in this thesis, during the scheduled period of study. I also declare that I have not taken any material from any source except referred to wherever due that amount of plagiarism is within acceptable range. If a violation of HEC rules on research project has occurred in this thesis, I shall be liable to punishable action under the plagiarism rules of the HEC.

Dated: _____

Signature of Student

_____

Amir Hassan

CIIT/SP20-RMT-025/LHR

Certificate

It is certified that Amir Hassan (CIIT/SP20-RMT-025/LHR) has carried out all the research work related to this thesis under my supervision at the Department of Mathematics, COMSATS University Islamabad, Lahore campus and the work fulfills the requirement for award of MS degree.

Dated: _____

Supervisor:

_____

Dr. Sana Javed
Assistant Professor

Head/Incharge of Department

_____

Dr. Kashif Ali
Associate Professor
Department of Mathematics

DEDICATIONS

My loving Parents, Teachers
and Friends who always encouraged
me to work hard and guided me towards
the right way and destination.

ACKNOWLEDGEMENTS

Words are limited to praise Allah Almighty who is the creator of the universe and bestowed upon me with the opportunity, courage and potential to complete this project. All best regards and praise after Allah Almighty are due to the Holy Prophet Hazrat Muhammad (PBUH), who is the greatest source of inspiration for all knowledge seekers.

Foremost, a very special thanks to my supervisor **Dr. Sana Javed** for her patience, encouragement, stimulating suggestions, constructive criticism and kind guidance during my research work. I would also express the thanks to **Dr. Kashif Ali** for well-maintained research environment. I take this opportunity to record my sincere thanks to all the faculty of Mathematics Department.

Moreover, I pay special thanks to a person, my well-wisher, my mentor, for his motivating attitude, who always support and encourage me when things seemed definitively stuck. This acknowledgement will be incomplete without mentioning my feelings for my loving parents, who sacrificed their comfort and happiness, just so that I could be happy and comfortable. It is impossible for me to achieve such a hard task without their support and priceless prayers. May **Allah** bless on them.

Amir Hassan
CIIT/SP20-RMT-025/LHR

ABSTRACT

The term used to illustrate a molecule/chemical compound in the form of graph is known as molecular/chemical graph. Molecules are usually represented as vertices while their bonding interaction is shown by edges in a molecular graph. In this thesis, we computed various connectivity indices based on degrees of vertices of chemical graph of Terbium Dioxide (TbO_2) and Graphitic Carbon Nitride (g-C_3N_4) including general Randic, ABC, GA and Zagreb indices etc. Afterwards, we found the physical measures like entropy and heat of formation of TbO_2 and g-C_3N_4. Then, we fitted curves between different indices and the thermodynamical properties namely heat of formation and entropy. Curve fitting was done in MATLAB through different methods based on linearity and non-linearity. The performance of the method was tested using root mean squared error (RMSE), the sum of squared errors (SSE) or R^2. Further, we gave graphical representations of these indices. These mathematical frameworks might provide a way to study the thermodynamics properties of the chemical structure of Terbium Dioxide (TbO_2) at intense level which will assist to comprehend the relationship between system dimension and these measures. This thesis is divided into five chapters. Chapter 1 includes the basic definition , notions and terminologies related to thesis. Chapter 2 provides a review of literature about out work .The main results are given in chapter 3 .Chapter 4 contains a brief discussion about the work while the chapter 5 consists of the references used in this thesis.

TABLE OF CONTENTS

Chapter 1

Introduction

1 Introduction

1.1 Graph Theory

The study of graphs, which are mathematical structures used to model pairwise relationships between things, is known as graph theory in mathematics. A graph is made up of vertices (also known as nodes) that are connected by edges (also called lines). Undirected graphs, in which edges might connect two vertices symmetrically, are distinguished from directed graphs, in which edges connect two vertices asymmetrically. Graphs are one of the most studied objects in discrete mathematics.

Graph theory has different implementations in many science fields including chemistry. Graph theoretical techniques provide the idea to study the molecular structures of chemical compounds at enormous level. These methods assist to understand the physical measures like entropy, enthalpy or heat of formation of chemical compounds as well as to approach the basic characteristics which necessitate the structure-property activity connection of molecules. This perspective permits to use mathematical formulation to understand the dynamics of a structure, as studying the structure through experiments is usually very costly and laborious. A chemical graph is a representation of a chemical compound where the compound elements like atoms or molecules are considered as nodes or vertices and the bonding or connection between two nodes is represented by a line called an edge. In molecular biology, graphs are often used to model and examine information with complex connections. Some basic definitions, notations and terms related to graphs are given in section 1.1.1.and 1.1.2.

1.1.1 Basic Notions and Terminologies

A *graph* $\mathcal{G}$ is a union of two sets, vertex set and edge set denoted by $\mathcal{V}$ and $\mathcal{E}$, respectively. In figure 1, $\{v_1, v_2, v_3, v_4\}$ represent vertex set while the $\{e_1, e_2, e_3, e_4\}$ represent the set of edges of graph $\mathcal{G}$. A graph having more than one edge between two vertices or loops on vertices is called a *multiple graph* otherwise a *simple graph*. Figure 1 represents a simple graph. The cardinalities of the sets $\mathcal{V}$ and $\mathcal{E}$ are called *order* and *size* of the graph $\mathcal{G}$. In figure 1, $\mathcal{V} = \{v_1, v_2, v_3, v_4\}$ and $\mathcal{E} = \{e_1, e_2, e_3, e_4\}$ imply both order and size of $\mathcal{G}$ is 4. Two vertices are called *adjacent* if they are incident to the same edge. A *path* is an alternate sequence of nodes and edges where nodes are joined by the edges and no edge is traversed more than once. The total number of edges contained in a path is regarded as the *length* of the path. A graph is called *connected* if it consists of only one component. There exists at least one path between every two vertices in a

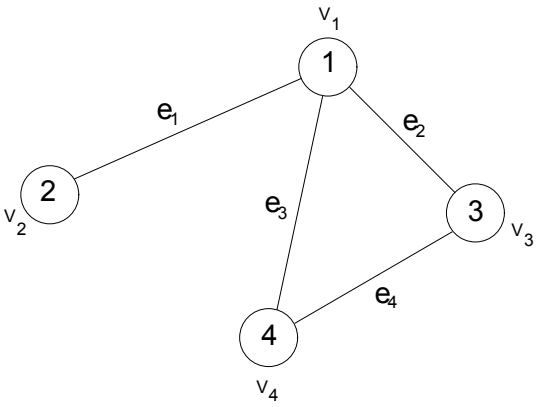

Figure 1: Simple Graph

connected graph. Two vertices might be connected by more than one path, the path having the shortest length defines the *distance* between two vertices. In figure 1, the vertices v_2 and v_3 are connected by two paths $\mathcal{P}_1 : v_2, e_1, v_1, e_3, v_4, e_4, v_3$ and $\mathcal{P}_2 : v_2, e_1, v_1, e_2, v_3$ where the length of $\mathcal{P}_1$ is 3 and the length of $\mathcal{P}_2$ is 2 so $d(v_2, v_3) = 2$. The total number of edges incident to a vertex v is called its *degree* and denoted by $\widetilde{\Im}(v)$. A graph *degree sequence* is composed of the sequence of degrees defined in an ascending order where the repetition is allowed. For instance, degree sequence of graph $\mathcal{G}$ in figure 1 is $(1, 2, 2, 3)$. Size (m) of a graph $\mathcal{G} = (\mathcal{V}, \mathcal{E})$ might be determined in the form of degrees by using the formula given below.

$$2m = \sum_{v \in \mathcal{G}} \widetilde{\Im}(v)$$

Two graphs are called *isomorphic* if their structure is preserved under an isomorphism. More precisely, if we can find a transformation which maps adjacent vertices of graph $\mathcal{G}$ to the adjacent vertices of graph $\mathcal{G}'$ then we say that $\mathcal{G}$ is isomorphic to $\mathcal{G}'$, symbolically it is written as $\mathcal{G} \cong \mathcal{G}'$. Figure 1 shows two isomorphic graphs $\mathcal{G}$ and $\mathcal{G}'$.

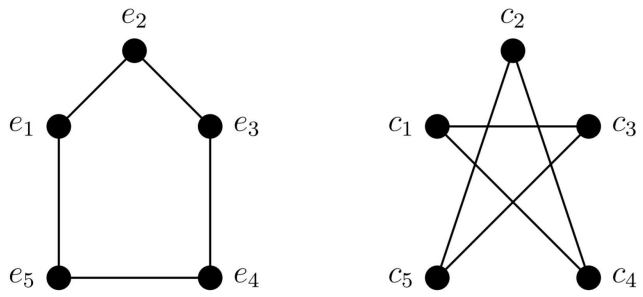

Figure 2: Isomorphic Graphs $\mathcal{G}$ and $\mathcal{G}'$

1.1.2 Topological Indices

Topological invariant presents a characteristics of graph which is found using just the abstract structure of the graph instead of using specific graph representation. Graph invariants are relatively used to study any graphical construction. Graph invariant is a numerical number that is purely estimated by the graph. Capturing the topology of the graph, under study, helps to study different chemical properties or activities connected with the graph structure. Such study is based on the graph invariants called *topological indices*. Any two isomorphic graphs share the same topological indices while the converse is not true. Connectivity indices are very valuable in studying the thermodynamical characteristics of compounds for example, entropy, heat formation, or enthalpy. Such quantifiable physical properties can be easily understood in the form of such connectivity indices which are directly computed using the graphical structure of the chemical compound under study A topological graph index, commonly referred to as molecular computing, is a mathematical formula that may be applied to any graph that represents a molecule structure. It is possible to examine mathematical values and explore various physical features of a molecule using this index. Therefore, it is an computational method used to avoid expensive and time-consuming laboratory experiments.

1.2 Chemical Terminologies

This subsection is concerned with the basic definitions, notions and terminologies from chemistry related to the main work of the thesis.

1.2.1 Chemical Compound

A material made of indistinguishable molecules comprising of atoms of more than one element is termed as *chemical compound*.

1.2.2 Terbium Dioxide

Rare earth oxide materials with f-electron systems that contain lanthanides and actinides series have a significant research interest due to their various applications out of which *terbium oxide* is the best and have fluorite-type RO2 (rare-earth dioxide) structure. Lanthanides have certain unique properties e.g, same physical properties in the series, preferably bind with most electronegative element, have very small crystal-field effects and little dependence on ligands. Terbium metal is the companion of lanthanide programme in table of element [22]. Terbium is

a light,malleable, ductile, silver-gray metal element of the periodic table lanthanide group. It is quite stable in the air, butit oxidises slowly and reacts to cold water. It is twice common as silver on earth crust and never present in free form.It has the most fascinating physical and chemical characteristics such as superconductivity at elevated temperatures,mixed valency, strong structural, magnetic, optical and electronic properties, etc [23]. Due to their exceptional catalytic properties, relatively high basicity and fast oxygen ion mobility, Rare earth metals have been discovered to be excellent possibilities for increasing sensing capabilities [24]. Tb doped ZnO is best known for VOCs (ethanol and acetone) sensing [25].

At room temperature, $TbO2$ forms a face-centered cubic structure (space group Fm3m) 3. Traditional terbium oxide synthesis relied on precipitation, however a recently developed SHS (self propagation high temperature synthesis) method produces a weakly agglomerated nanosized powder of terbium oxide. Thermo chemical water splitting utilizes extreme temperatures and chemical reactions to produce hydrogen andlow-cost, full-color flat-panel displays of the next generation [31]. An effective EL system specifically requires the high performance of photoluminescence (PL) materials, thermal stability, and mobility of the charge carrier. Since their photoluminescence has high quantum efficiency and a sharp spectral band, rare earth complexes are theoretically worthy of EL use [32]. Rare earth metals have their partially filled inner f-orbital that are surrounded by 5p and 5s orbitals that are totally filled kind of covering provides transition of f-electrons that gives optical emission of radiations ranging from ultraviolet to the infrared [33]. Rare earth metals are of great interest due to the transitions in their ions that gives wide range of colors. Intense green electroluminescence of Tb ions makes it more attractive in multicolor light emitting devices as compared to the simple silicon based light emitting devices.The enhanced electroluminescence is due to the transition in Tb ions, wide band gap and the constant of the lattice (10.73°A) parallel to Si (5.431°A) [34].

This electroluminescence can be enhanced by the addition of a organic ligand to terbium ions. Mostly its electroluminescence is affected by the structure of the pyrazolone derivative central ligands and the N- or oxygen from water, from solar energy or from the exhaust gases of nuclear power reactions. This is a long-term process in technology, with potentially little to no emissions of greenhouse gases. All chemical solvents used in the method can be fully recycled; the only consumption is water, while the only production is H2 and O2 [27]. To date, thermo chemical One of the more appealing methods of water splitting is by redox metal oxide reactions long-term techniques of generating reusable Fuel cells can use H2 directly as well as additional conversion to fuel cells. This method has a number of advantages: I The top cycle temperature

(usually around 12001600 C) is consistent with long-term concentrated solar power; (ii) simple inputs including water and heat are safe chemical solutions; (iii)Various reactions separate the H2 and O2 streams produced; (iv) The closed cycle recycles the chemicals and reactants on a continuous basis; (v) The H2 produced is pure enough to be processed directly, such as in a polymer electrolyte membrane fuel cell (PEMFC) [28]. Terbium oxide is involved in the thermo chemical hydrogen production Tb-WS (thermochemical water splitting) is a two-stage solar thermochemical water splitting cycle. The thermal reduction of TbO2 into Tb and O2 is the first phase of the cycle, The second stage produces H2 by oxidising Tb through a water splitting process [29]. Electroluminescence refers to the creation of light (luminescence) by a medium in response to the electrical current flowing through the medium [30]. Effective thin film organic or conjugated polymericmaterial based electroluminescence (EL) devices are a promising candidate forO-containing neutral ligands due to their ligand-to-metal energy transfer [35].

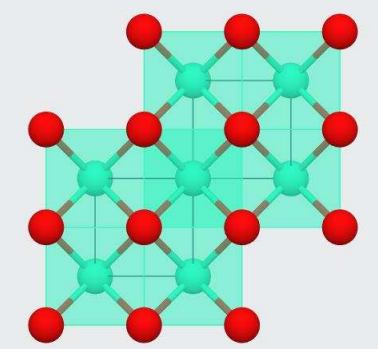

Figure 3: Structure of Terbium Dioxide

1.2.3 Graphitic Carbon Nitride

Graphitic carbon nitrides ($g-C_3N_4$) is a family of 2D polymer substance. It is a solid structure made up of triazine or tris-s-triazine building blocks with sp2 hybridised C and N atoms in alternate positions [30]. The atoms are arranged in such a way that each C atom is bound by the three closest N atoms, two N atoms established bonds with three others adjoining atoms of C can be seen in figure 4. The feature constitution such as $g-C_3N_4$ have a huge contentment of N pyridinic spaces unify dispense, six lone-pair electrons of nitrogen in so-called'nitrogen Pots', it is ideal model locations for coordination and stabilisation [12].

Direct moisture of organic precursors containing urea, such as nitrogen, guanidine hydrochloride and cyanamide is typically used to produce carbon nitride compounds. Due to its great thermal and chemical solidity, powerless and appropriate preparation, and outstanding electrical charac-

teristics, graphitic carbon nitride ($g - C_3N_4$), has gotten a lot of attention as an effective photo catalyst [2]. Graphite Carbon Nitride $g-C_3N_4$'s semiconductor nature has remind huge strength to improve photo (electro)chemical efficiencies in structure design operate point in a reachable endless energy history [26].

1.2.4 Thermodynamical Properties of Chemical Compound

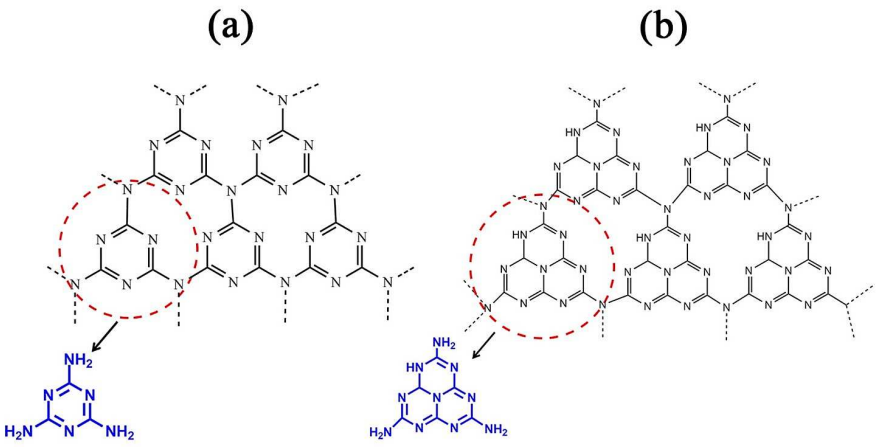

Figure 4: (a) Triazine and (b) Tri-s-triazine (Heptazine) Structures of $g - C_3N_4$ [29, 31].

To construct a thermodynamical structure we need to measure some physical quantities including heat of formation and entropy.

Entropy

Entropy measure tells us how much heat energy we need to produce more in order to perform some valued work. Since this measure is describing the lack of energy due to which performing valuable work is not possible so it is also termed as measure of disorder [12, 14]. The entropy of an isolated system has the highest entropy, according to the second law of thermodynamics. Non-isolated systems can lose entropy if they enhance the entropy of their surroundings by at least the same amount. Because entropy is a state function, every process that moves a system from one state to another, whether reversible or irreversible, will change its entropy.

Heat of Formation

During per unit formation, the heat absorbed or retained is referred as *heat of formation* provided all the elements persist in normal state. Kilojoules per mole (kJ/mol) is the unit for the measure of $\mathcal{H}o\mathcal{F}$. The term enthalpy is also used for $\mathcal{H}o\mathcal{F}$.

1.3 Chemical Graph

The term used to illustrate a molecule/chemical compound in the form of a graph is known as *molecular/chemical* graph [7, 17]. Molecules are shown as vertices while their bonding or interactions are shown by edges in a molecular graph. Mostly molecule graphs are simple graphs and the measure of topological index is invariant under graph isomorphisms. Mostly, the degree or distance measure is used to capture the topology of a graphical structure so the most common indices are based on either degree or distance between the vertices. Indices comprising of degree measurements perform a vigorous part in molecular graph theory. Two isomorphic graphs have same connectivity indices and the cardinalities of vertex and edge sets of a graph are considered as topological/connectivity indices as well. A connectivity index explains some helpful details about structure and analysis of a molecular graph.

1.4 Mathematical Model

Defining a system in the form of a mathematical framework provides us an efficient approach to analyze the dynamics of the system. Experimental work is mostly expensive and very time consuming so transforming the system into a set of mathematical form makes this study very coherent. Many softwares like MATLAB or Python are easily available which provide a very friendly environment to construct mathematical models and study them.

1.5 Statistical Tests

As we may fit many mathematical models to the same set of data so making a choice is difficult which one is best suited to us. There are several statistical tests which might help us to decide which mathematical model or framework is a best fit for our data. Few of these tests are stated here. Let (X, Y) be a data set containing m observations. Suppose Y is the output variable while X is input-data. Let *f(X)* be the set of corresponding fitted values of Y .

1.5.1 Mean Squared Error

The mean squared error ($\mathcal{MSE}$) is defined in (1).

$$\mathcal{MSE} = \frac{1}{m} \sum_{(x,y)\in(X,Y)} (y - f(x))^2 \tag{1}$$

1.5.2 Sum of Squared Error

The sum of squared error ($\mathcal{SSE}$) is defined in (2).

$$\mathcal{SSE} = \sum_{(x,y)\in(X,Y)} (y - f(x))^2 \tag{2}$$

1.5.3 $\mathcal{R}^2$-Test

$\mathcal{R}^2$-test explains how much scatter the observed values are from our fitted line or curve. The value closer to 1 indicates a good fit while value closer to zero indicates a poor estimate. Let $\mathcal{S}$ be the variance defined by the fit and φ be the total variance then $\mathcal{R}^2$ is defined by the formula given in (3).

$$R^2 = \frac{\mathcal{S}}{\varphi} \tag{3}$$

1.5.4 Root Mean Squared Error

The root mean squared error ($\mathcal{RMSE}$) is defined in (4.)

$$\mathcal{RMSE} = \sqrt{\frac{1}{m} \sum_{(x,y)\in(X,Y)} (y - f(x))^2} \tag{4}$$

There are several other statistical tests available in the literature but we will just consider $\mathcal{RMSE}$, $\mathcal{SSE}$ or $\mathcal{R}^2$.

1.6 Confidence Interval

A confidence is a range of values that estimates for an unknown parameter, defined as an interval with a lower bound and an upper bound. The interval is calculated at a designated confidence level. The most common confidence level is 95 percent.

Chapter 2

Literature Review

2 Literature Review

The role of graph theory is vital in studying the chemical properties of a specific chemical structure. In particular, the topological or connectivity indices assist to identify the underlying topology of a chemical compound which helps to study different properties or chemical activities of molecules associated with their chemical configuration. Lately, various chemical compounds have been explored utilizing their corresponding visual representation based on their fundamental topology. A chemical graph is a visualization of a molecular substance that elucidates its components and their coordination, components are shown as points and lines are utilized to show associations between chemical components.

Terbium, a lanthanide, is a light, malleable, ductile, silver-gray metal element of the periodic table. TbO_2 at room temperature exhibits a face-centered cubic structure.. The objective of this study is to determine relationships between the thermodynamical properties and the topological indices of TbO_2. Such relationships might provide insights to comprehend the structural ons of TbO_2.

Graph theory has many applications in various science disciplines, specifically biology, chemistry and computer science. It provides a way to illustrate any structure or compound in a graphical form which helps to study the interrelated behavior of chemical components. It provides a deep insight how the chemical components or molecules are related and influence each other. Graph invariants are frequently used to study any graphical structure. Graph invariant is a numerical number that is exclusively evaluated by the graph. Comprehension with the topology of the graph, under consideration, helps us to study different chemical properties or activities interrelated with the graph structure. Such study is conducted based on the graph invariants called topological indices. Any two isomorphic graphs share the same topological indices while the converse is not true. Connectivity indices are very worthwhile in studying the thermodynamical properties of chemical compounds for instance, entropy, boiling points, heat of formation, or enthalpy. Such measurable physical properties can be easily understood in the form of such connectivity indices which are directly computed using the graphical structure of the chemical compound under consideration.

The first zagreb index $\mathcal{M}_1(\mathcal{G})$ was the first index presented in 1972 by Gutman to illustrate the connection between graphs and orbital shapes which was further extended in 2004 and named as the second zagreb index $\mathcal{M}_2(\mathcal{G})$. There are many other degree based indices as well; few of them are listed here. Suppose $\mathcal{G} = (\mathcal{V}, \mathcal{E})$ denote a graph with $\mathcal{V}$ representing the set of vertices

and $\mathcal{E}$ representing the set of edges. The degree $\widetilde{\Im}(s)$ of a vertex s is the number of edges of $\mathcal{G}$ incident with s.

The first and most well-known degree-based index was created by Milan Randic [32] in 1975 and can be found in the equation below.

$$\mathcal{R}_{-\frac{1}{2}}(\mathcal{G}) = \sum_{st\in\mathcal{E}(\mathcal{G})} \frac{1}{\sqrt{\widetilde{\Im}(s)\times\widetilde{\Im}(t)}}$$

In 1988, Bollobás *el at.* [9] and Amic *et al.* [3] proposed the general Randić index exclusively. For more details about Randić index, its properties and important results see [13, 28]. The general Randić index is defined as:

$$\mathcal{R}_{\alpha}(\mathcal{G}) = \sum_{st\in\mathcal{E}(\mathcal{G})} (\widetilde{\Im}(s)\times\widetilde{\Im}(t))^{\alpha}$$

Estrada et al. established the atom bond connectivity index in [17]. It is defined as:

$$\mathcal{ABC}(\mathcal{G}) = \sum_{st\in\mathcal{E}(\mathcal{G})} \sqrt{\frac{\widetilde{\Im}(s)+\widetilde{\Im}(t)-2}{\widetilde{\Im}(s)\times\widetilde{\Im}(t)}}$$

The geometric arithmetic index $\mathcal{GA}$ of a graph $\mathcal{G}$ was created by Vukičević *et al.* [37]. It is defined as:

$$\mathcal{GA}(\mathcal{G}) = \sum_{st\in E(\mathcal{G})} \frac{2\sqrt{\widetilde{\Im}(s)\times\widetilde{\Im}(t)}}{\widetilde{\Im}(s)+\widetilde{\Im}(t)}$$

The first and second Zagreb indices are written as following:

$$\mathcal{M}_1(\mathcal{G}) = \sum_{st\in\mathcal{E}(\mathcal{G})} (\widetilde{\Im}(s)+\widetilde{\Im}(t))$$

$$\mathcal{M}_2(\mathcal{G}) = \sum_{st\in\mathcal{E}(\mathcal{G})} (\widetilde{\Im}(s)\times\widetilde{\Im}(t))$$

In 2008, Došlić defined the first Zagreb coindex and second Zagreb coindex in [19], as following:

$$\overline{\mathcal{M}_1}(\mathcal{G}) = \sum_{st\notin\mathcal{E}(\mathcal{G})} [\widetilde{\Im}(s)+\widetilde{\Im}(t)]$$

$$\overline{\mathcal{M}_2}(\mathcal{G}) = \sum_{st\notin\mathcal{E}(\mathcal{G})} (\widetilde{\Im}(s)\times\widetilde{\Im}(t))$$

In 2013, Shirdel, *et al.* [19] introduced a new degree-based Zagreb index namely hyper-Zagreb index as given below:

$$\mathcal{HM}(\mathcal{G}) = \sum_{st \in \mathcal{E}(\mathcal{G})} \left[\widetilde{\mathfrak{F}}(s) + \widetilde{\mathfrak{F}}(t)\right]^2$$

In 2012, Ghorbani and Azimi, [24] defined two new versions of Zagreb indices of a graph $\mathcal{G}$. The first multiple Zagreb index . $\mathcal{PM}_1(\mathcal{G})$ and second multiple Zagreb index $\mathcal{PM}_2(\mathcal{G})$ and these indices are defined as:

$$\mathcal{PM}_1(\mathcal{G}) = \prod_{st \in \mathcal{E}(\mathcal{G})} [\widetilde{\mathfrak{F}}(s) + \widetilde{\mathfrak{F}}(t)]$$

$$\mathcal{PM}_2(\mathcal{G}) = \prod_{st \in \mathcal{E}(\mathcal{G})} [\widetilde{\mathfrak{F}}(s) \times \widetilde{\mathfrak{F}}(t)]$$

Furtula and Gutman, [18] presented forgotten topological index which was characterized as follows:

$$\mathcal{F}(\mathcal{G}) = \sum_{st \in \mathcal{E}(\mathcal{G})} \left(\widetilde{\mathfrak{F}}(s)^2 + \widetilde{\mathfrak{F}}(t)^2\right)$$

Spurred by the achievement of the $\mathcal{ABC}$ index, Furtula set forth its changed adaptation, [5, 6] and they named as augmented Zagreb index and is characterized as:

$$\mathcal{AZI}(\mathcal{G}) = \sum_{st \in \mathcal{E}(\mathcal{G})} \left(\frac{\widetilde{\mathfrak{F}}(s) \times \widetilde{\mathfrak{F}}(t)}{\widetilde{\mathfrak{F}}(s) + \widetilde{\mathfrak{F}}(t) - 2}\right)^3$$

Another topological index based on the vertex degree is the Balaban index. This index for a graph $\mathcal{G}$ of order k, size l is defined as

$$\mathcal{J}(\mathcal{G}) = \frac{l}{l-k+2} \sum_{st \in \mathcal{E}(\mathcal{G})} \frac{1}{\sqrt{\widetilde{\mathfrak{F}}(s) \times \widetilde{\mathfrak{F}}(t)}}$$

The redefined version of the Zagreb indices were defined by Ranjini *et al.* [33] called, the redefined first, second and third redefined Zagreb indices. These indices are presented as follows:

$$\begin{aligned}
\mathcal{R}e\mathcal{Z}\mathcal{G}_1(\mathcal{G}) &= \sum_{st\in\mathcal{E}(\mathcal{G})} \frac{\widetilde{\Im}(s)+\widetilde{\Im}(t)}{\widetilde{\Im}(s)\times\widetilde{\Im}(t)} \\
\mathcal{R}e\mathcal{Z}\mathcal{G}_2(\mathcal{G}) &= \sum_{st\in\mathcal{E}(\mathcal{G})} \frac{\widetilde{\Im}(s)\times\widetilde{\Im}(t)}{\widetilde{\Im}(s)+\widetilde{\Im}(t)} \\
\mathcal{R}e\mathcal{Z}\mathcal{G}_3(\mathcal{G}) &= \sum_{st\in\mathcal{E}(\mathcal{G})} \widetilde{\Im}(s)\times\widetilde{\Im}(t)(\widetilde{\Im}(s)+\widetilde{\Im}(t))
\end{aligned}$$

Chapter 3

Main Results

3 Main Results

This chapter contains the main results of this thesis. Section 3.1 provides the results regarding the chemical graph of terbium dioxide including computations of various topological indices and different thermodynamical properties of TbO_2 and graphical models between topological indices and physical properties.

3.1 Terbium Dioxide

3.1.1 Topological Indices of TbO_2

The number of vertices and edges of structure of TbO_2 are $22lk$ and $32lk$, respectively. Since there are three type of vertices in TbO_2 namely the vertices of degree 1, 2, 4, respectively. The vertex partition of the vertex set TbO_2 is presented in table 1. Also the edge partition of TbO_2 based on degrees of end vertices of each edge are depicted in table 2. Let $\mathcal{G} = (\mathcal{V}, \mathcal{E})$ denotes

Table 1: Vertex partition of TbO_2 based on degree of vertex

$\widetilde{\Im}(s)$	Frequency	Set of Vertices
1	$4lk + 4$	$\mathcal{V}_1$
2	$2k + 2l - 4$	$\mathcal{V}_2$
4	$18lk - 2l - 2k$	$\mathcal{V}_3$

Table 2: Edge partition of TbO_2

$(\widetilde{\Im}(s),\ \widetilde{\Im}(t))$	Frequency	Set of Edges
$(1, 4)$	$12lk - 2k - 2l$	$\mathcal{E}_1$
$(2, 4)$	$4lk - 2l - 2k$	$\mathcal{E}_2$
$(4, 4)$	$16lk + 4k + 4l$	$\mathcal{E}_3$

the chemical graph of TbO_2, and suppose that $\widetilde{\Im}(s)$ denotes the degree of the vertex s.

- $\mathcal{R}_\alpha$ index of TbO_2

For $\alpha = 1$,

$$\begin{aligned}
\mathcal{R}_1(\mathcal{G}) &= \sum_{st \in \mathcal{E}(\mathcal{G})} (\widetilde{\Im}(s) \times \widetilde{\Im}(t)) \\
&= (12lk - 2k - 2l)(1 \times 4) + (4lk - 2l - 2k)(2 \times 4) + (16lk + 4k + 4l)(4 \times 4) \\
&= 336lk + 40l + 40k
\end{aligned}$$

For $\alpha = -1$,

$$\begin{aligned}
\mathcal{R}_{-1}(\mathcal{G}) &= \sum_{st\in\mathcal{E}(\mathcal{G})} \frac{1}{(\widetilde{\Im}(s)\times\widetilde{\Im}(t))} \\
&= (12lk-2k-2l)\frac{1}{(1\times 4)} + (4lk-2l-2k)\frac{1}{(2\times 4)} + (16lk+4l+4k)\frac{1}{(4\times 4)} \\
&= \frac{9lk-l-k}{2}.
\end{aligned}$$

For $\alpha = \frac{1}{2}$,

$$\begin{aligned}
\mathcal{R}_{\frac{1}{2}}(\mathcal{G}) &= \sum_{st\in\mathcal{E}(\mathcal{G})} \sqrt{(\widetilde{\Im}(s)\times\widetilde{\Im}(t))} \\
&= (12lk-2k-2l)(2) + (4lk-2l-2k)(2\sqrt{2}) + (16lk+4l+4k)(4) \\
&= 88lk+12l+12k+(8lk-4l-4k)(\sqrt{2})
\end{aligned}$$

For $\alpha = -\frac{1}{2}$,

$$\begin{aligned}
\mathcal{R}_{-\frac{1}{2}}(\mathcal{G}) &= \sum_{st\in\mathcal{E}(\mathcal{G})} \frac{1}{\sqrt{(\widetilde{\Im}(s)\times\widetilde{\Im}(t))}} \\
&= (12lk-2k-2l)\frac{1}{\sqrt{(1\times 4)}} + (4lk-2k-2l)\frac{1}{\sqrt{(2\times 4)}} + (16lk+4l+4k)\frac{1}{\sqrt{(4\times 4)}} \\
&= (12lk-2k-2l)\frac{1}{(2)} + (4lk-2l-2k)\frac{1}{(2\sqrt{2})} + (16lk+4l+4k)\frac{1}{(4)} \\
&= 10lk+(2lk-l-k)\frac{1}{(\sqrt{2})}
\end{aligned}$$

The numerical representation of above computed results are presented in table 3.

Graphical illustrations of Randic indices are provided in figure 5.

Table 3: Randic indices for $\alpha \in \{1, -1, \frac{1}{2}, -\frac{1}{2}\}$

$[\boldsymbol{l}, \boldsymbol{k}]$	$\mathcal{R}_1(\mathcal{G})$	$\mathcal{R}_{-1}(\mathcal{G})$	$\mathcal{R}_{\frac{1}{2}}(\mathcal{G})$	$\mathcal{R}_{-\frac{1}{2}}(\mathcal{G})$
$[1,1]$	416	3.5	112	10
$[2,2]$	1504	16	416	42.828
$[3,3]$	3264	37.5	912	98.485
$[4,4]$	5696	68	1600	176.971
$[5,5]$	8800	107.5	2480	278.284
$[6,6]$	12576	156	3552	402.426
$[7,7]$	17024	213.5	4816	549.397

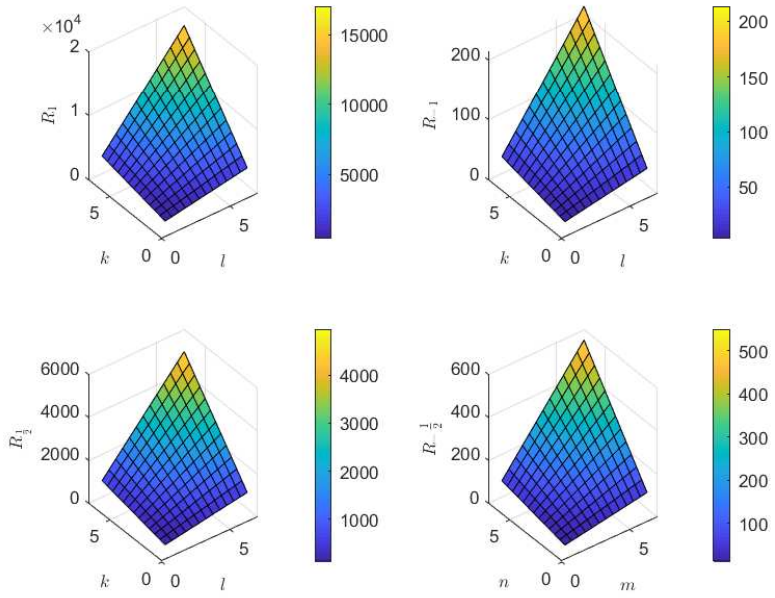

Figure 5: Graphical Representation of Randic Indices

- $\mathcal{ABC}$ index of TbO_2

The result for $\mathcal{ABC}$ index is follows as:

$$\begin{aligned}
\mathcal{ABC}(\mathcal{G}) &= \sum_{st\in\mathcal{E}(\mathcal{G})}\sqrt{\frac{\widetilde{\Im}(s)+\widetilde{\Im}(t)-2}{d_s d_t}} \\
&= (12lk-2k-2l)\Big(\sqrt{\frac{1+4-2}{1\times 4}}\Big)+(4lk-2l-2k)\Big(\sqrt{\frac{2+4-2}{2\times 4}}\Big) \\
&+ (16lk+4l+4k)\Big(\sqrt{\frac{4+4-2}{4\times 4}}\Big) \\
&= (12lk-2k-2l)\Big(\sqrt{\frac{3}{4}}\Big)+(4lk-2l-2k)\Big(\sqrt{\frac{1}{2}}\Big)+(16lk+4l+4k)\Big(\sqrt{\frac{3}{8}}\Big)
\end{aligned}$$

- $\mathcal{GA}$ index of TbO_2

The $\mathcal{GA}$ index is computed as below:

$$\begin{aligned}
\mathcal{GA}(\mathcal{G}) &= \sum_{st\in E(\mathcal{G})} \frac{2\sqrt{\widetilde{\Im}(s)\times\widetilde{\Im}(t)}}{\widetilde{\Im}(s)+\widetilde{\Im}(t)} \\
&= (12lk-2k-2m)\Big(\frac{2\sqrt{1\times 4}}{1+4}\Big)+(4lk-2l-2k)\Big(\frac{2\sqrt{2\times 4}}{2+4}\Big) \\
&+ (16lk+4l+4k)\Big(\frac{2\sqrt{4\times 4}}{4+4}\Big) \\
&= (12lk-2k-2l)\Big(\frac{4}{5}\Big)+(4lk-2l-2k)\Big(\frac{2\sqrt{2}}{3}\Big)+(16lk+4l+4k)
\end{aligned}$$

The numerical representation of above computed results are presented in table 4. Graphical

Table 4: $\mathcal{ABC}$ and $\mathcal{GA}$ indices for TbO_2.

$[\boldsymbol{l},\boldsymbol{k}]$	$\mathcal{ABC}(\mathcal{G})$	$\mathcal{GA}(\mathcal{G})$
$[1,1]$	21.625	30.4
$[2,2]$	89.288	119.5425
$[3,3]$	202.988	267.4274
$[4,4]$	362.725	474.0548
$[5,5]$	568.499	739.425
$[6,6]$	820.312	1063.537
$[7,7]$	1118.161	1446.392

illustrations of $\mathcal{ABC}(\mathcal{G})$ and $\mathcal{GA}(\mathcal{G})$ indices are provided in figure 6.

- $\mathcal{M}_1$ and $\mathcal{M}_2$ indices of TbO_2

The first and second Zagreb indices are computed as below:

$$\begin{aligned}
\mathcal{M}_1(\mathcal{G}) &= \sum_{st\in\mathcal{E}(\mathcal{G})} (\widetilde{\Im}(s)+\widetilde{\Im}(t)) \\
&= (12lk-2k-2l)(1+4)+(4lk-2l-2k)(2+4)+(16lk+4l+4k)(4+4) \\
&= 212lk-+10k+10l.
\end{aligned}$$

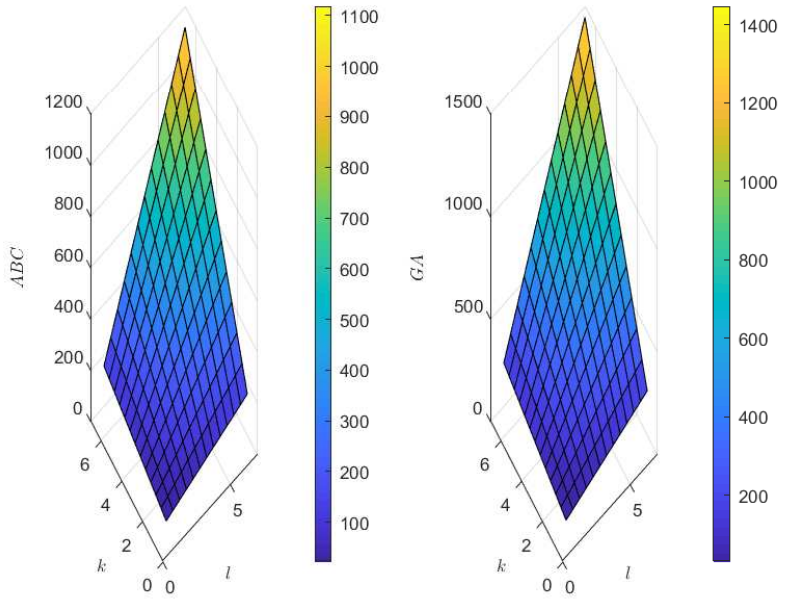

Figure 6: Graphical Representations of $\mathcal{ABC}(\mathcal{G})$ and $\mathcal{GA}(\mathcal{G})$ Indices

$$\begin{aligned}
\mathcal{M}_2(\mathcal{G}) &= \sum_{st\in\mathcal{E}(\mathcal{G})} (\widetilde{\Im}(s)\times\widetilde{\Im}(t)) \\
&= (12lk-2k-2l)(1\times 4)+(4lk-2l-2k)(2\times 4) \\
&+ (16lk+4l+4k)(4\times 4) \\
&= 208lk+8k+8l.
\end{aligned}$$

- $\overline{\mathcal{M}_1}$ and $\overline{\mathcal{M}_2}$ of TbO_2

The first and second Zagreb co-indices are computed as below:

$$\begin{aligned}
\overline{\mathcal{M}_1}(\mathcal{G}) &= \sum_{pq\notin\mathcal{E}(\mathcal{G})} (\widetilde{\Im}(s)+\widetilde{\Im}(t)) \\
&= 2(32lk)(24lk)-(212lk+10k+10l) \\
&= 15364l^2k^2-212lk-10l+10k.
\end{aligned}$$

$$\begin{aligned}
\overline{\mathcal{M}_2}(\mathcal{G}) &= \sum_{pq \notin \mathcal{E}(\mathcal{G})} (\widetilde{\Im}(s) \times \widetilde{\Im}(t)) \\
\overline{\mathcal{M}_2}(\mathcal{G}) &= 2(24lk)^2 - \frac{1}{2}(212lk + 10k + 10l) - (208lk + 8k + 8l) \\
&= 1152l^2k^2 - 314lk - 13k - 13l.
\end{aligned}$$

The above-mentioned computed results are represented numerically are presented in table 5. Graphical illustrations of $\mathcal{ABC}(\mathcal{G})$ and $\mathcal{GA}$ indices are provided in figure 7.

Table 5: $\mathcal{M}_1(\mathcal{G})$, $\mathcal{M}_2(\mathcal{G})$, $\overline{\mathcal{M}_1}(\mathcal{G})$, $\overline{\mathcal{M}_2}(\mathcal{G})$ indices for TbO_2.

$[\boldsymbol{l}, \boldsymbol{k}]$	$\mathcal{M}_1(\mathcal{G})$	$\mathcal{M}_2(\mathcal{G})$	$\overline{\mathcal{M}_1}(\mathcal{G})$	$\overline{\mathcal{M}_2}(\mathcal{G})$
$[1, 1]$	232	224	15152	812
$[2, 2]$	888	864	244976	17124
$[3, 3]$	1968	1920	1242576	90408
$[4, 4]$	3472	3392	3929792	289784
$[5, 5]$	5400	5280	9597200	712020
$[6, 6]$	7752	7584	19904112	1481532
$[7, 7]$	10528	10304	36878576	2750384

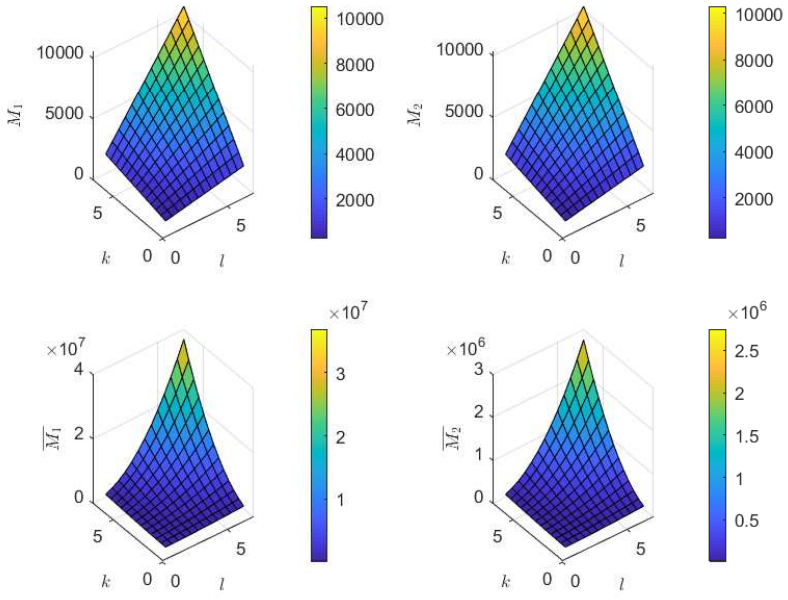

Figure 7: Graphical Representations of $\mathcal{ABC}$ and $\mathcal{GA}$ Indices

- The $\mathcal{HM}$ index of TbO_2

The hyper Zagreb index is calculated as follows:

$$\begin{aligned}
\mathcal{HM}(\mathcal{G}) &= \sum_{st\in\mathcal{E}(\mathcal{G})} \big(\widetilde{\Im}(s)+\widetilde{\Im}(t)\big)^2 \\
\mathcal{HM}(\mathcal{G}) &= (12lk-2k-2l)\big(1+4\big)^2+(4lk-2l-2k)\big(2+4\big)^2 \\
&+ (16lk+4l+4k)\big(4+4\big)^2 \\
\mathcal{HM}(\mathcal{G}) &= 4540lk+902l+902k.
\end{aligned}$$

The numerical representation of above computed result is presented in table 6.

Graphical illustration of $\mathcal{HM}(\mathcal{G})$ index is provided in figure 8.

Table 6: $\mathcal{HM}(\mathcal{G})$ for TbO_2

$[\boldsymbol{l},\boldsymbol{k}]$	$\mathcal{HM}(\mathcal{G})$
$[1,1]$	6344
$[2,2]$	21768
$[3,3]$	46272
$[4,4]$	79856
$[5,5]$	122520
$[6,6]$	174264
$[7,7]$	235088

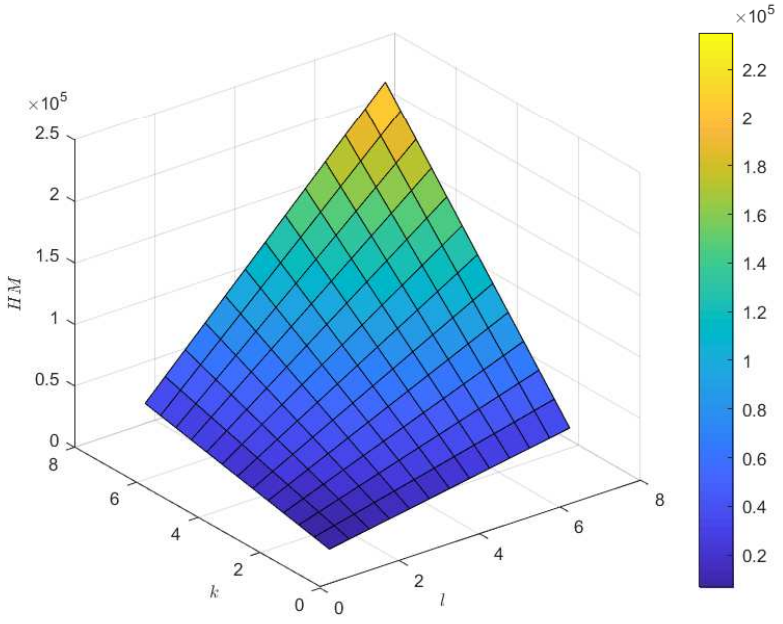

Figure 8: Graphical Representations of $\mathcal{HM}(\mathcal{G})$ Index

- $\mathcal{F}$ index of TbO_2

The Forgotten index is calculated as:

$$\begin{aligned}
\mathcal{F}(\mathcal{G}) &= \sum_{st\in\mathcal{E}(\mathcal{G})} \left(\widetilde{\Im}(s)^2 + \widetilde{\Im}(t)^2\right) \\
&= (12lk-2k-2l)((1)^2+(4)^2) + (4lk-2l-2k)((2)^2+(4)^2) + (16lk+4l+4k)((4)^2+(4)^2) \\
&= (12lk-2k-2l)(17) + (4lk-2l-2k)(20) + (16lk+4l+4k)(32) \\
&= 796lk + 54l + 54k.
\end{aligned}$$

- $\mathcal{AZ}$ index of TbO_2

The augmented Zagreb index is calculated as below:

$$\begin{aligned}
\mathcal{AZI}(\mathcal{G}) &= \sum_{st\in\mathcal{E}(\mathcal{G})} \left(\frac{\widetilde{\Im}(s)\times\widetilde{\Im}(t)}{\widetilde{\Im}(s)+\widetilde{\Im}(t)-2}\right)^3 \\
&= \sum_{st\in\mathcal{E}_1} \left(\frac{1\times 4}{1+4-2}\right)^3 + \sum_{st\in\mathcal{E}_2} \left(\frac{2\times 4}{2+4-2}\right)^3 + \sum_{st\in\mathcal{E}_3} \left(\frac{4\times 4}{4+4-2}\right)^3 \\
&= \frac{64}{27}(12lk-2k-2l) + 8(4lk-2l-2k) + \frac{512}{27}(16lk+4l+4k) \\
&= \frac{9824lk}{27} + \frac{496l}{9} + \frac{496k}{9}.
\end{aligned}$$

- $\mathcal{J}$ index of Tbo_2

The Balaban index is computes as:

$$\begin{aligned}
\mathcal{J}(\mathcal{G}) &= \frac{q}{q-p+2} \sum_{st\in\mathcal{E}(\mathcal{G})} \frac{1}{\sqrt{\widetilde{\Im}(s)\times\widetilde{\Im}(t)}} \\
&= \frac{q}{q-p+2} \left[\sum_{st\in\mathcal{E}_1} \frac{1}{\sqrt{1\times 4}} + \sum_{st\in\mathcal{E}_2} \frac{1}{\sqrt{2\times 4}} + \sum_{st\in\mathcal{E}_3} \frac{1}{\sqrt{4\times 4}}\right] \\
&= \frac{22lk}{10lk-2} \times \left[\frac{1}{2}(12lk-2k-2l) + \frac{1}{2\sqrt{2}}(4lk-2l-2k) + \frac{1}{4}(16lk+4l+4k)\right]
\end{aligned}$$

The above-mentioned computed findings are numerically represented in table 7. Graphical illustrations of $\mathcal{F}(\mathcal{G})$, $\mathcal{AZI}(\mathcal{G})$ and $\mathcal{J}(\mathcal{G})$ indices are provided in figure 9.

- $\mathcal{ReZG}_1$, $\mathcal{ReZG}_2$ and $\mathcal{ReZG}_3$ indices of TbO_2

Table 7: $\mathcal{F}(\mathcal{G})$, $\mathcal{AZI}(\mathcal{G})$, $J(\mathcal{G})$ indices for TbO_2.

$[\boldsymbol{l}, \boldsymbol{k}]$	$\mathcal{F}(\mathcal{G})$	$\mathcal{AZI}(\mathcal{G})$	$\mathcal{J}(\mathcal{G})$
$[1, 1]$	904	474.07	27.5
$[2, 2]$	3400	1675.85	99.18
$[3, 3]$	7488	3605.33	221.59
$[4, 4]$	13168	6262.52	394.26
$[5, 5]$	20440	9647.41	617.16
$[6, 6]$	29304	13760	890.28
$[7, 7]$	39760	18600.3	1213.63

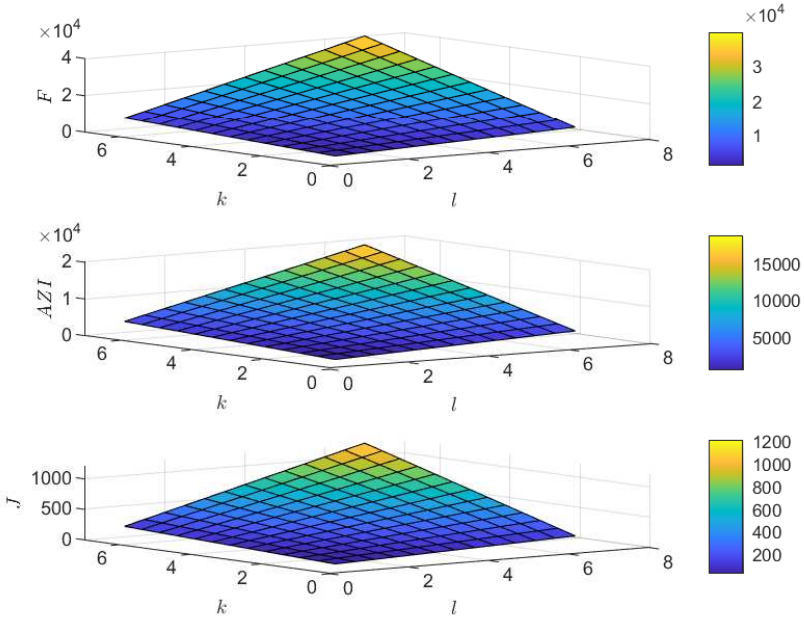

Figure 9: Graphical Representations of $\mathcal{F}(\mathcal{G})$, $\mathcal{AZI}(\mathcal{G})$ and $\mathcal{J}(\mathcal{G})$ Indices

The redefined Zagreb indices are computed as:

$$\begin{aligned}
\mathcal{ReZG}_1(\mathcal{G}) &= \sum_{st\in\mathcal{E}(\mathcal{G})} \frac{\widetilde{\mathfrak{F}}(s)+\widetilde{\mathfrak{F}}(t)}{\widetilde{\mathfrak{F}}(s)\times\widetilde{\mathfrak{F}}(t)} \\
&= \sum_{st\in\mathcal{E}_1} \frac{1+4}{1\times 4} + \sum_{st\in\mathcal{E}_2} \frac{2+4}{2\times 4} + \sum_{st\in\mathcal{E}_3} \frac{4+4}{4\times 4} \\
&= \frac{5}{4}(12lk-2k-2l) + \frac{3}{4}(4lk-2l-2k) + \frac{1}{2}(16lk+4l+4k)).
\end{aligned}$$

$$\begin{aligned}
\mathcal{R}e\mathcal{Z}\mathcal{G}_2(\mathcal{G}) &= \sum_{st\in\mathcal{E}(\mathcal{G})} \frac{\widetilde{\Im}(s)\times\widetilde{\Im}(t)}{\widetilde{\Im}(s)+\widetilde{\Im}(t)} \\
&= \sum_{st\in\mathcal{E}_1} \frac{1\times 4}{1+4} + \sum_{st\in\mathcal{E}_2} \frac{2\times 4}{2+4} + \sum_{st\in\mathcal{E}_3} \frac{4\times 4}{4+4} \\
&= \frac{4}{5}(12lk-2k-2l) + \frac{4}{3}(4lk-2l-2k) + (2)(16lk+4l+4k)).
\end{aligned}$$

$$\begin{aligned}
\mathcal{R}e\mathcal{Z}\mathcal{G}_3(\mathcal{G}) &= \sum_{st\in\mathcal{E}(\mathcal{G})} [\widetilde{\Im}(s)\widetilde{\Im}(t)(\widetilde{\Im}(s)+\widetilde{\Im}(t))] \\
&= 20(12lk-2k-2l) + 48(4lk-2l-2k) + 128(16lk+4l+4k) \\
&= 2480lk + 376l + 376k.
\end{aligned}$$

The numerical representations of above computed results are presented in table 8. Graphical

Table 8: $\mathcal{R}e\mathcal{Z}\mathcal{G}_1(\mathcal{G}), \mathcal{R}e\mathcal{Z}\mathcal{G}_2(\mathcal{G}), \mathcal{R}e\mathcal{Z}\mathcal{G}_3(\mathcal{G})$ indices for TbO_2

$[\boldsymbol{l}, \boldsymbol{k}]$	$\mathcal{R}e\mathcal{Z}\mathcal{G}_1(\mathcal{G})$	$\mathcal{R}e\mathcal{Z}\mathcal{G}_2(\mathcal{G})$	$\mathcal{R}e\mathcal{Z}\mathcal{G}_3(\mathcal{G})$
$[1,1]$	22	54.4	3232
$[2,2]$	96	202.67	11424
$[3,3]$	222	444.8	24576
$[4,4]$	400	780.8	42688
$[5,5]$	630	1210.67	65760
$[6,6]$	912	1734.4	93792
$[7,7]$	1246	2352	126784

illustrations of $\mathcal{R}e\mathcal{Z}\mathcal{G}_1(\mathcal{G})$, $\mathcal{R}e\mathcal{Z}\mathcal{G}_2(\mathcal{G})$ and $\mathcal{R}e\mathcal{Z}\mathcal{G}_3(\mathcal{G})$ indices are provided in figure 10.

3.1.2 $\mathcal{H}o\mathcal{F}$ and *Entropy* of TbO_2

The topological indices $\mathcal{R}_1$, $\mathcal{R}_{-1}$, $\mathcal{R}_{\frac{1}{2}}$, $\mathcal{R}_{-\frac{1}{2}}$, $\mathcal{ABC}$, $\mathcal{GA}$, $\mathcal{M}_1$, $\mathcal{M}_2$, $\overline{\mathcal{M}_1}$ and $\overline{\mathcal{M}_2}$ etc were determined for various numbers of unit cells of TbO_2. These indices are linked to the thermodynamic characteristics of TbO_2 such as entropy and heat of formation. TbO_2 has a standard molar $\mathcal{H}o\mathcal{F}$ of $18.70kJmol^{-1}(4.47kcal/mol)$ the standard molar $\mathcal{H}o\mathcal{F}$ for one formula unit was obtained by dividing it with Avogadro's number. The $\mathcal{H}o\mathcal{F}$ of the complete cell was calculated by multiplying the obtained value by the number of formula units contained in the cell. The $\mathcal{H}o\mathcal{F}$ of TbO_2 has an inverse relationship with its crystal size, decreasing as the number of unit cells increases, according to these calculations. The entropy of polycyclic graphite carbon nitride was calculated using the same approach. TbO_2 has a molar standard *Entropy* of $77Jmol^{-1}K^{-1}$. The result was then multiplied by the number of formula units present in a single unit cell. The value of

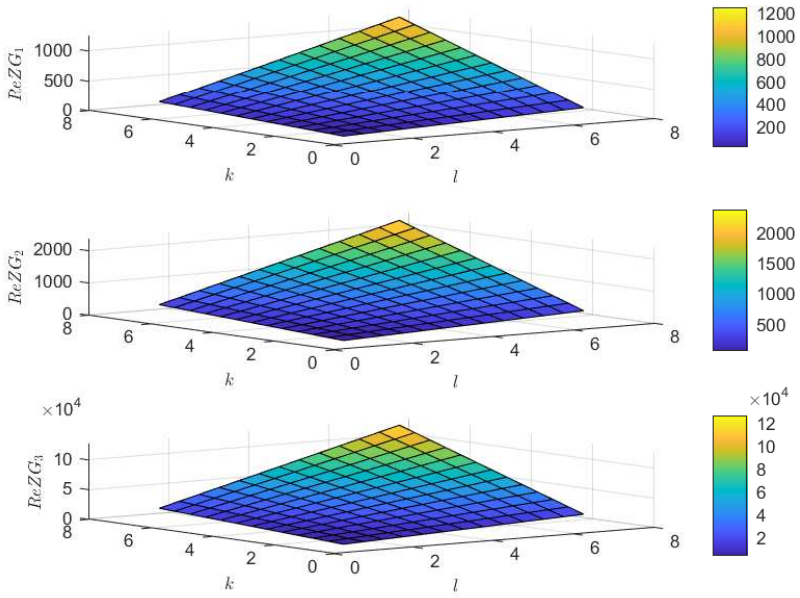

Figure 10: Graphical Representations of $\mathcal{R}e\mathcal{Z}\mathcal{G}_1(\mathcal{G})$, $\mathcal{R}e\mathcal{Z}\mathcal{G}_2(\mathcal{G})$ and $\mathcal{R}e\mathcal{Z}\mathcal{G}_3(\mathcal{G})$ Indices

entropy falls as the number of cells increases. The same downward trend can be seen in the heat of creation.

The entropy and $\mathcal{H}o\mathcal{F}$ of TbO_2 for $1 \leq l \leq 7$ and $1 \leq k \leq 7$ matching to various formula units are computed in table 9 as follows: Since degree-base indices, as well as the accompanying entropy

Table 9: $\mathcal{H}o\mathcal{F}$, Entropy values corresponding to various formula units of TbO_2

$[\boldsymbol{l}, \boldsymbol{k}]$	Formula units	Entropy $\times 10^{22} kJ$	$\mathcal{H}o\mathcal{F} \times 10^{22} kJ$
$[1, 1]$	4	1.2462	5.1316
$[2, 2]$	16	4.9850	20.5264
$[3, 3]$	36	11.2162	46.1846
$[4, 4]$	64	19.9400	82.1059
$[5, 5]$	100	31.1562	128.2905
$[6, 6]$	144	44.8650	184.7384
$[7, 7]$	196	61.0663	251.44951

and $\mathcal{H}o\mathcal{F}$, have a wide range of applications in science, including pharmaceutical, chemistry, biological therapies, and computer science. So graphical and numerical representation can benefit the scientists from these calculated outcomes.

3.1.3 Curve Fitting of $\mathcal{H}o\mathcal{F}$ (and Entropy) vs Topological Indices

We can study the link between several variables to a set of data. This analysis is performed to investigate the relationship between $\mathcal{H}o\mathcal{F}$/entropy and topological indices. Curve fitting methods

have been implemented to find this link. ($\mathcal{RMSE}$), sum of squared error ($\mathcal{SSE}$) and $\mathcal{R}^2$ are accuracy measures used in the analysis. The rational (rat) strategy has produced the best outcomes in every situation. MATLAB was used to do all of the simulations. Tables 10-11 present the errors for each fit.

3.1.4 Models for Indices vs $\mathcal{HoF}$

Graphical models of $\mathcal{HoF}$ vs indices are shown in figures 11-27.

$$\mathcal{HoF}(\mathcal{R}_1) = \frac{p_1 \times (\mathcal{R}_1) + p_2}{(\mathcal{R}_1)^3 + q_1^2 \times (\mathcal{R}_1) + q_2 + q_3},$$

where $(\mathcal{R}_1)$ is normalized by mean 7040 and std 6110

Parametric values (alongside 95% $\mathcal{CI}$):

$p_1 = -2558$, $\mathcal{CI}= (-3680, -1436)$

$p_2 = -2927$, $\mathcal{CI}= (-4205, -1648)$

$q_1 = -2.136$, $\mathcal{CI}= (-2.393, -1.88)$

$q_2 = 1.809$, $\mathcal{CI}= (1.128, 2.49)$

$q_3 = -118$, $\mathcal{CI}= (-169.6, -66.32)$

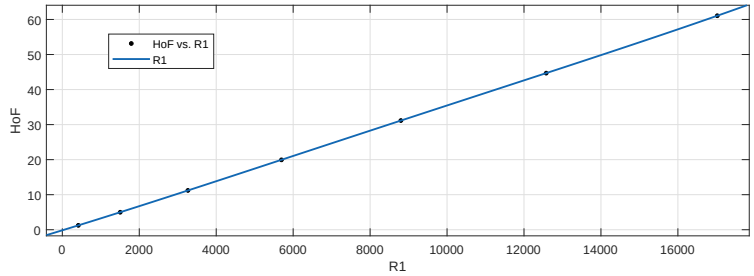

Figure 11: $\mathcal{HoF}$ vs $\mathcal{R}_1$

$$\mathcal{HoF}((R_{-1}) = \frac{p_1 \times (R_{-1}) + p_2}{(R_{-1})^4 + q_1 \times (R_{-1})^3 + q_2 \times (R_{-1})^2 + q_3 \times (R_{-1}) + q_4},$$

where $(\mathcal{R}_{-1})$ is normalized by mean 86 and std 77.46.

Parametric values (alongside 95% $\mathcal{CI}$):

$p_1 = -2767$, $\mathcal{CI}= (-6440, 904.8)$

$p_2 = -3093$, $\mathcal{CI}= (-7207, 1021)$

$q_1 = -1.854$, $\mathcal{CI}= (-2.53, -1.177)$

$q_2 = 0.8569$, $\mathcal{CI}= (-0.6522, 2.366)$

$q_3 = -1.957$, $\mathcal{CI}= (-5.415, 1.5)$

$q_4 = -123.4$, $\mathcal{CI}= (-287.5, 40.63)$

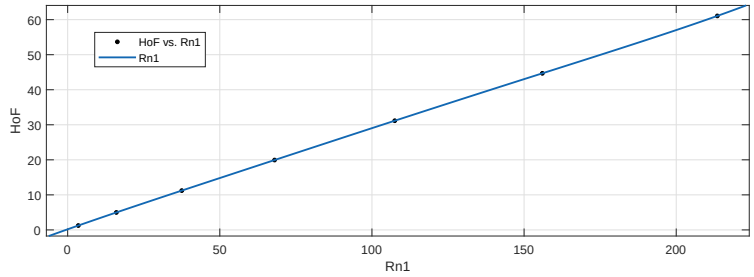

Figure 12: $\mathcal{HoF}$ vs $\mathcal{R}_{-1}$

$$\mathcal{HoF}(R_{\frac{1}{2}}) = \frac{p_1 \times (\mathcal{R}_{\frac{1}{2}}) + p_2}{(\mathcal{R}_{\frac{1}{2}})^4 + q_1 \times (\mathcal{R}_{\frac{1}{2}})^3 + q_2 \times (\mathcal{R}_{\frac{1}{2}})^2 + q_3 \times (R_{\frac{1}{2}}) + q_4},$$

where $(\mathcal{R}_{\frac{1}{2}})$ is normalized by mean 1984 and std 1731

Parametric values (alongside 95% $\mathcal{CI}$):

$p_1 = 6.405e+05$, $\mathcal{CI}= (-1.351e+09, 1.352e+09)$

$p_2 = 7.32e+05$, $\mathcal{CI}= (-1.544e+09, 1.545e+09)$

$q_1 = -263.5$, $\mathcal{CI}= (-5.519e+05, 5.514e+05)$

$q_2 = 544.6$, $\mathcal{CI}= (-1.148e+06, 1.149e+06)$

$q_3 = -381.3$, $\mathcal{CI}= (-8.06e+05, 8.052e+05)$

$q_4 = 2.946e+04$, $\mathcal{CI}= (-6.212e+07, 6.218e+07)$

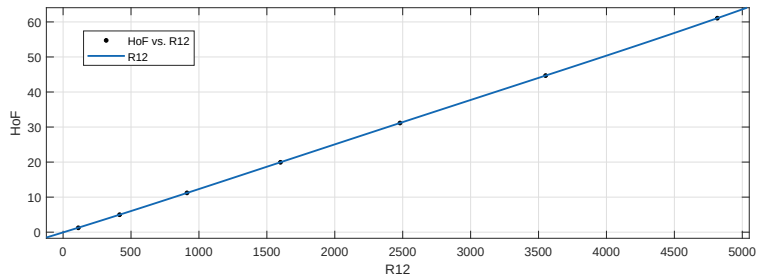

Figure 13: $\mathcal{HoF}$ vs $\mathcal{R}_{\frac{1}{2}}$

$$\mathcal{H}o\mathcal{F}(\mathcal{R}_{-\frac{1}{2}}) = \frac{p_1 \times (\mathcal{R}_{-\frac{1}{2}}) + p_2}{(\mathcal{R}_{-\frac{1}{2}})^4 + q_1 \times (\mathcal{R}_{-\frac{1}{2}})^3 + q_2 \times (\mathcal{R}_{-\frac{1}{2}})^2 + q_3 \times (\mathcal{R}_{-\frac{1}{2}}) + q_4},$$

where $(\mathcal{R}_{-\frac{1}{2}})$ is normalized by mean 222.6 and std 198.8

Parametric values (alongside 95% $\mathcal{CI}$):

$p_1 = 5.987e+05$, $\mathcal{CI}= (-1.347e+09, 1.348e+09)$

$p_2 = 6.741e+05$, $\mathcal{CI}= (-1.517e+09, 1.518e+09)$

$q_1 = -100.9$, $\mathcal{CI}= (-2.226e+05, 2.224e+05)$

$q_2 = 46.26$, $\mathcal{CI}= (-1.033e+05, 1.034e+05)$

$q_3 = 317.7$, $\mathcal{CI}= (-7.136e+05, 7.142e+05)$

$q_4 = 2.695e+04$, $\mathcal{CI}= (-6.062e+07, 6.067e+07)$

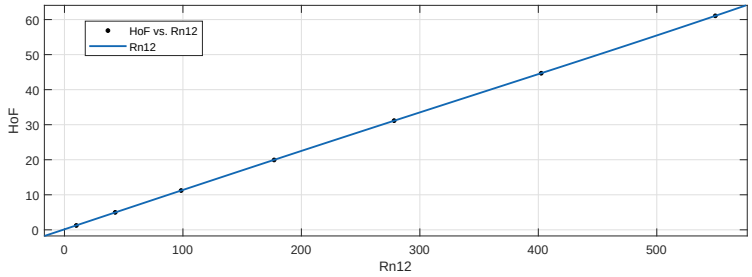

Figure 14: $\mathcal{H}o\mathcal{F}$ vs $\mathcal{R}_{-\frac{1}{2}}$

$$\mathcal{H}o\mathcal{F}(\mathcal{ABC}) = \frac{p_1 + p_2}{(\mathcal{ABC})^4 + q_1 \times (\mathcal{ABC})^3 + q_2 \times (\mathcal{ABC})^2 + q_3 \times (\mathcal{ABC}) + q_4},$$

where $(\mathcal{ABC})$ is normalized by mean 454.8 and std 404.1

Parametric values (alongside 95% $\mathcal{CI}$):

$p_1 = 9.075e+05$, $\mathcal{CI}= (-3.302e+09, 3.304e+09)$

$p_2 = 1.023e+06$, $\mathcal{CI}= (-3.722e+09, 3.724e+09)$

$q_1 = -130.8$, $\mathcal{CI}= (-4.686e+05, 4.683e+05)$

$q_2 = 41.11$, $\mathcal{CI}= (-1.483e+05, 1.484e+05)$

$q_3 = 399.3$, $\mathcal{CI}= (-1.451e+06, 1.452e+06)$

$q_4 = 4.095e+04$, $\mathcal{CI}= (-1.49e+08, 1.491e+08)$

$$\mathcal{H}o\mathcal{F}(\mathcal{GA}) = \frac{p_1 \times (\mathcal{GA}) + p_2}{(\mathcal{GA})^4 + q_1 \times (\mathcal{GA})^3 + q_2 \times (\mathcal{GA})^2 + q_3 \times (\mathcal{GA}) + q_4},$$

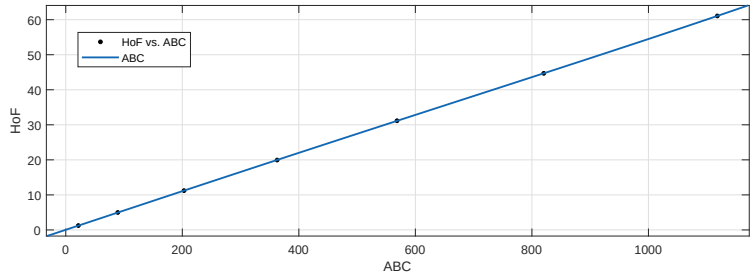

Figure 15: $\mathcal{HoF}$ vs $\mathcal{ABC}$

where ($\mathcal{GA}$) is normalized by mean 591.5 and std 521.5. Parametric values (alongside 95% $\mathcal{CI}$):

$p_1 = 6.295e+05$, $\mathcal{CI}= (-9.53e+08, 9.543e+08)$

$p_2 = 7.138e+05$, $\mathcal{CI}= (-1.081e+09, 1.082e+09)$

$q_1 = -164.5$, $\mathcal{CI}= (-2.462e+05, 2.459e+05)$

$q_2 = 248.1$, $\mathcal{CI}= (-3.751e+05, 3.756e+05)$

V $q_3 = -1.624$, $\mathcal{CI}= (-3409, 3406)$

$q_4 = 2.864e+04$, $\mathcal{CI}= (-4.336e+07, 4.341e+07)$

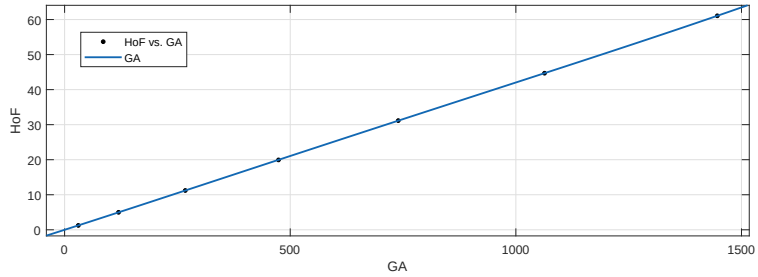

Figure 16: $\mathcal{HoF}$ vs $\mathcal{GA}$

$$\mathcal{HoF}(\mathcal{M}_1) = \frac{p_1 \times (\mathcal{M}_1) + p_2}{(\mathcal{M}_1)^3 + q_1 \times (\mathcal{M}_1)^2 + q_2 \times (\mathcal{M}_1) + q_3},$$

where is normalized by mean 4320 and std 3791.

Parametric values (alongside 95% $\mathcal{CI}$):

$p_1 = -3341$, $\mathcal{CI}= (-5810, -872.7)$

$p_2 = -3799$, $\mathcal{CI}= (-6597, -1001)$

$q_1 = -1.772$, $\mathcal{CI}= (-2.281, -1.262)$

$q_2 = 0.7253$, $\mathcal{CI}= (-0.178, 1.629)$

$q_3 = -152.7$, $\mathcal{CI}= (-265.3, -40.01)$

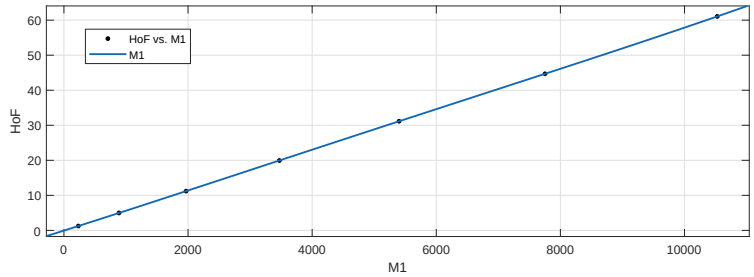

Figure 17: $\mathcal{H}o\mathcal{F}$ vs $\mathcal{M}_1$

$$\mathcal{H}o\mathcal{F}(\mathcal{M}_2) = \frac{p_1 \times (\mathcal{M}_1) + p_2}{(\mathcal{M}_1)^3 + q_1 \times (\mathcal{M}_1)^2 + q_2 \times (\mathcal{M}_1) + q_3},$$

where $(\mathcal{M}_2)$ is normalized by mean 4224 and std 3712.

Parametric values (alongside 95% $\mathcal{CI}$):

$p_1 = -3473$, $\mathcal{CI}= (-6278, -668.8)$

$p_2 = -3946$, $\mathcal{CI}= (-7123, -770)$

$q_1 = -1.71$, $\mathcal{CI}= (-2.295, -1.126)$

$q_2 = 0.5448$, $\mathcal{CI}= (-0.4644, 1.554)$

$q_3 = -158.5$, $\mathcal{CI}= (-286.3, -30.68)$

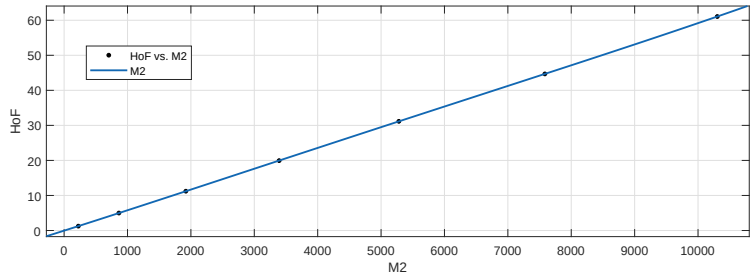

Figure 18: $\mathcal{H}o\mathcal{F}$ vs $\mathcal{M}_2$

$$\mathcal{H}o\mathcal{F}(\overline{\mathcal{M}_1}) = \frac{p_1 \times (\mathcal{M}_2) + p_2}{(\mathcal{M}_2)^4 + q_1 \times (\mathcal{M}_2)^3 + q_2 \times (\mathcal{M}_2)^2 + q_3 \times (\mathcal{M}_2) + q_4},$$

where $(\overline{\mathcal{M}_1})$ is normalized by mean $1.026e+07$ and std $1.372e+07$.

Parametric values (alongside 95% $\mathcal{CI}$):

$p_1 = 9.12e+05$, $\mathcal{CI}= (-5.922e+10, 5.922e+10)$

$p_2 = 6.923e+05$, $\mathcal{CI}= (-4.495e+10, 4.495e+10)$

$q_1 = 2091$, $\mathcal{CI}= (-1.359e+08, 1.359e+08)$

$q_2 = -6936$, $\mathcal{CI}= (-4.503e+08, 4.503e+08)$

$q_3 = 1.51e+04$, $\mathcal{CI}= (-9.801e+08, 9.801e+08)$

$q_4 = 2.186e+04$, $\mathcal{CI}= (-1.419e+09, 1.419e+09)$

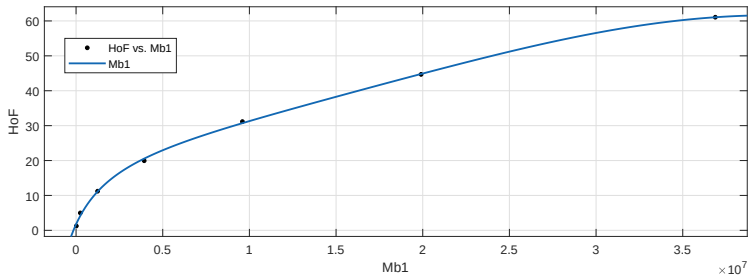

Figure 19: $\mathcal{H}o\mathcal{F}$ vs $\overline{\mathcal{M}_1}$

$$\mathcal{H}o\mathcal{F}(\overline{\mathcal{M}_2}) = \frac{p_1 \times (\overline{\mathcal{M}_2}) + p_2}{(\overline{\mathcal{M}_2})^3 + q_1 \times (\overline{\mathcal{M}_2})^2 + q_2 \times (\overline{\mathcal{M}_2}) + q_3},$$

where $(\overline{\mathcal{M}_2})$ is normalized by mean $7.632e+05$ and std $1.023e+06$

Parametric values (alongside 95% $\mathcal{CI}$):

$p_1 = -2.416e+06$, $\mathcal{CI}= (-6.719e+10, 6.719e+10)$

$p_2 = -1.896e+06$, $\mathcal{CI}= (-5.271e+10, 5.27e+10)$

$q_1 = 5874$, $\mathcal{CI}= (-1.634e+08, 1.634e+08)$

$q_2 = -3.721e+04$, $\mathcal{CI}= (-1.035e+09, 1.035e+09)$

$q_3 = -5.77e+04$, $\mathcal{CI}= (-1.604e+09, 1.604e+09)$

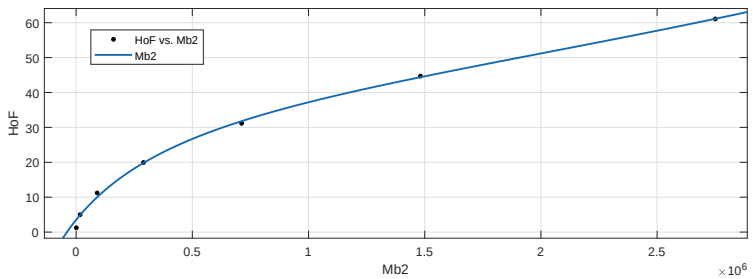

Figure 20: $\mathcal{H}o\mathcal{F}$ vs $\overline{\mathcal{M}_2}$

$$\mathcal{H}o\mathcal{F}(\mathcal{HM}) = \frac{p_1 \times (\mathcal{HM}) + p_2}{(\mathcal{HM})^2 + q_1 \times (\mathcal{HM}) + q_2},$$

where $(\mathcal{HM})$ is normalized by mean $9.802e+04$ and std $8.409e+04$.

Parametric values (alongside 95% $\mathcal{CI}$):

$p_1 = 8345$, $\mathcal{CI}= (-2.846e+04, 4.515e+04)$

$p_2 = 9564$, $\mathcal{CI}= (-3.254e+04, 5.166e+04)$

$q_1 = -6.927$, $\mathcal{CI}= (-29.01, 15.15)$

$q_2 = 388.1$, $\mathcal{CI}= (-1319, 2096)$

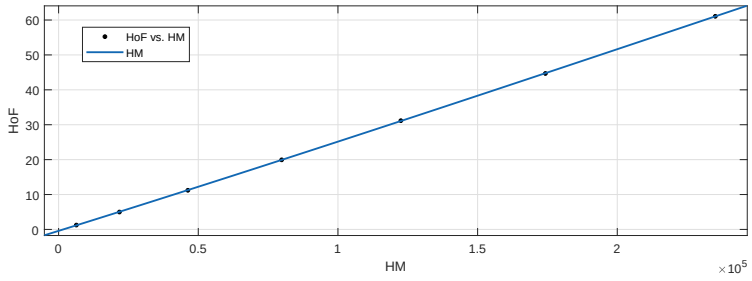

Figure 21: $\mathcal{H}o\mathcal{F}$ vs $\mathcal{HM}$

$$\mathcal{H}o\mathcal{F}(\mathcal{F}) = \frac{p_1 \times (\mathcal{F}) + p_2}{(\mathcal{F})^4 + q_1 \times (\mathcal{F})^3 + q_2 \times (\mathcal{F})^2 + q_3 \times (\mathcal{F}) + q_4},$$

where $(\mathcal{F})$ is normalized by mean $1.635e+04$ and std $1.43e+04$.

Parametric values (alongside 95% $\mathcal{CI}$):

$p_1 = 6.763e+05$, $\mathcal{CI}= (-1.435e+09, 1.437e+09)$

$p_2 = 7.691e+05$, $\mathcal{CI}= (-1.632e+09, 1.634e+09)$

$q_1 = -183.3$, $\mathcal{CI}= (-3.85e+05, 3.846e+05)$

$q_2 = 317.8$, $\mathcal{CI}= (-6.738e+05, 6.744e+05)$

$q_3 = -165.1$, $\mathcal{CI}= (-3.519e+05, 3.516e+05)$

$q_4 = 3.094e+04$, $\mathcal{CI}= (-6.566e+07, 6.572e+07)$

$$\mathcal{H}o\mathcal{F}(\mathcal{AZI}) = \frac{p_1 \times (\mathcal{AZI}) + p_2}{(\mathcal{AZI})^4 + q_1 \times (\mathcal{AZI})^3 + q_2 \times (\mathcal{AZI})^2 + q_3 \times (\mathcal{AZI}) + q_4},$$

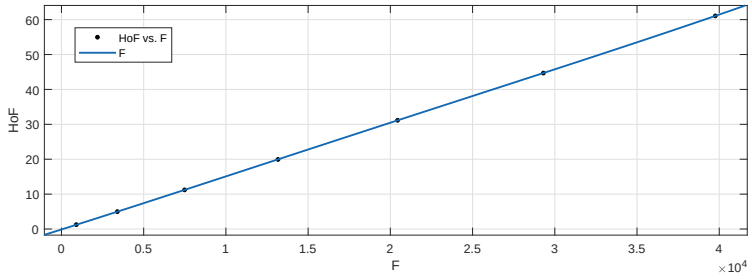

Figure 22: $\mathcal{HOF}$ vs $\mathcal{F}$

where $(\mathcal{AZI})$ is normalized by mean 7718 and std 6667.

Parametric values (alongside 95% $\mathcal{CI}$):

$p_1 = 3.228e+05$, $\mathcal{CI}= (-1.699e+08, 1.706e+08)$

$p_2 = 3.704e+05$, $\mathcal{CI}= (-1.95e+08, 1.957e+08)$

$q_1 = -140.3$, $\mathcal{CI}= (-7.305e+04, 7.277e+04)$

$q_2 = 311.3$, $\mathcal{CI}= (-1.637e+05, 1.643e+05)$

$q_3 = -297$, $\mathcal{CI}= (-1.572e+05, 1.566e+05)$

$q_4 = 1.495e+04$, $\mathcal{CI}= (-7.871e+06, 7.901e+06)$

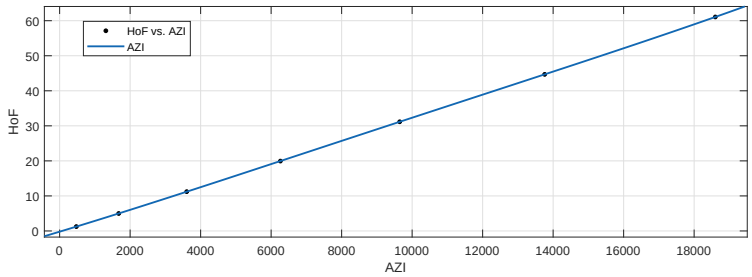

Figure 23: $\mathcal{HOF}$ vs $\mathcal{AZI}$

$$\mathcal{HOF}(\mathcal{J}) = \frac{p_1 \times (\mathcal{J}) + p_2}{(\mathcal{J})^3 + q_1 \times (\mathcal{J})^2 + q_2 \times (\mathcal{J}) + q_3},$$

where $(\mathcal{J})$ is normalized by mean 494.8 and std 437.4.

Parametric values (alongside 95% $\mathcal{CI}$):

$p_1 = 8.218e+05$, $\mathcal{CI}= (-4.139e+08, 4.156e+08)$

$p_2 = 9.235e+05$, $\mathcal{CI}= (-4.652e+08, 4.67e+08)$

$q_1 = -237$, $\mathcal{CI}= (-1.188e+05, 1.183e+05)$

$q_2 = 569.3$, $\mathcal{CI}= (-2.864e+05, 2.875e+05)$

$q_3 = 3.695e+04$, $\mathcal{CI}= (-1.861e+07, 1.868e+07)$

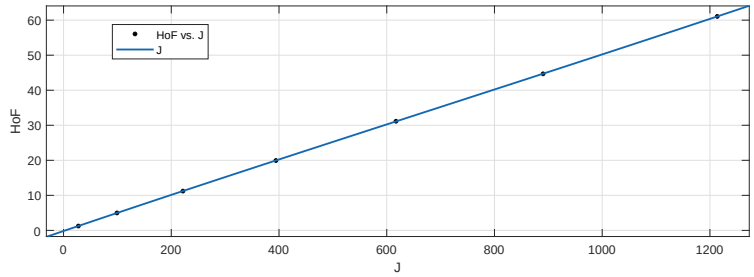

Figure 24: $\mathcal{H}o\mathcal{F}$ vs $\mathcal{J}$

$$\mathcal{H}o\mathcal{F}(\mathcal{R}e\mathcal{Z}\mathcal{G}_1) = \frac{p_1 \times (\mathcal{R}e\mathcal{Z}\mathcal{G}_1) + p_2}{(\mathcal{R}e\mathcal{Z}\mathcal{G}_1)^3 + q_1 \times (\mathcal{R}e\mathcal{Z}\mathcal{G}_1)^2 + q_2 \times (\mathcal{R}e\mathcal{Z}\mathcal{G}_1) + q_3},$$

where $(\mathcal{R}e\mathcal{Z}\mathcal{G}_1)$ is normalized by mean 504 and std 451.3.

Parametric values (alongside 95% $\mathcal{CI}$):

$p_1 = -7616$, $\mathcal{CI}= (-3.294e+04, 1.771e+04)$

$p_2 = -8560$, $\mathcal{CI}= (-3.698e+04, 1.986e+04)$

$q_1 = 0.1822$, $\mathcal{CI}= (-7.732, 8.096)$

$q_2 = -5.012$, $\mathcal{CI}= (-24.72, 14.7)$

$q_3 = -341.9$, $\mathcal{CI}= (-1478, 794.4)$

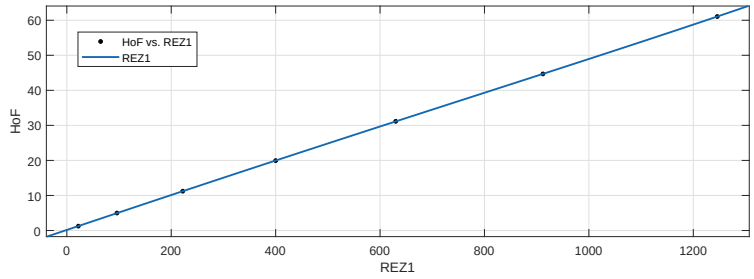

Figure 25: $\mathcal{H}o\mathcal{F}$ vs $\mathcal{R}e\mathcal{Z}\mathcal{G}_1$

$$\mathcal{H}o\mathcal{F}(\mathcal{R}e\mathcal{Z}\mathcal{G}_2) = \frac{p_1 \times (\mathcal{R}e\mathcal{Z}\mathcal{G}_2)^2 + p_2 \times (\mathcal{R}e\mathcal{Z}\mathcal{G}_2) + p_3}{(\mathcal{R}e\mathcal{Z}\mathcal{G}_2) + q_1},$$

where $(\mathcal{R}e\mathcal{Z}\mathcal{G}_2)$ is normalized by mean 968.5 and std 845.7.

Parametric values (alongside 95% $\mathcal{CI}$):

$p_1 = 21.8$, $\mathcal{CI}= (21.14, 22.47)$

$p_2 = -23.57$, $\mathcal{CI}= (-110.4, 63.31)$

$p_3 = -54.85$, $\mathcal{CI}= (-153, 43.27)$

$q_1 = -2.21$, $\mathcal{CI}= (-6.172, 1.752)$

$q_3 = -106.8$, $\mathcal{CI}= (-298.8, 85.1)$

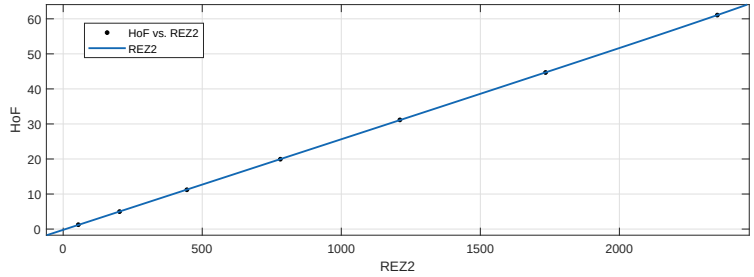

Figure 26: $\mathcal{HoF}$ vs $\mathcal{ReZG}_2$

$$\mathcal{HoF}(\mathcal{ReZG}_3) = \frac{p_1 \times (\mathcal{ReZG}_3)^2 + p_2 \times (\mathcal{ReZG}_3) + p_3}{(\mathcal{ReZG}_3)^3 + q_1 \times (\mathcal{ReZG}_3)^2 + q_2 \times (\mathcal{ReZG}_3) + q_3},$$

where $(\mathcal{ReZG}_3)$ is normalized by mean $5.261e+04$ and std $4.544e+04$.

Parametric values (alongside 95% $\mathcal{CI}$):

$p_1 = 88.95$ $(-8718, 8896)$

$p_2 = -2204$ $(-1.404e+04, 9633)$

$p_3 = -2646$ $(-7390, 2098)$

$q_1 = -2.302$ $(-7.697, 3.092)$

$q_2 = 6.274$ $(-402.5, 415.1)$

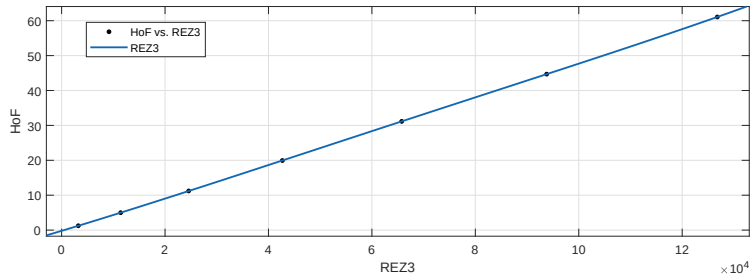

Figure 27: $\mathcal{HoF}$ vs $\mathcal{ReZG}_3$

Table 10: Goodness of Fit for $\mathcal{H}o\mathcal{F}$ vs indices for TbO_2

Index	Fit Type	$\mathcal{SSE}$	$\mathcal{R}^2$	$\mathcal{RMSE}$
$\mathcal{R}_1$	rat13	0.000394	1	0.01397
$\mathcal{R}_{-1}$	rat14	4.287e-05	1	0.006547
$\mathcal{R}_{\frac{1}{2}}$	rat14	0.001768	1	0.04204
$\mathcal{R}_{-\frac{1}{2}}$	rat14	0.00248	1	0.0498
$\mathcal{ABC}$	rat14	0.002838	1	0.05327
$\mathcal{GA}$	rat14	0.0009871	1	0.03142
$\mathcal{M}_1$	rat13	0.0006736	1	0.01835
$\mathcal{M}_2$	rat13	0.0007479	1	0.01934
$\overline{\mathcal{M}_1}$	rat14	1.6585	0.9994	1.298
$\overline{\mathcal{M}_2}$	rat13	7.392	0.9975	1.923
$\mathcal{HM}$	rat12	0.02971	1	0.09951
$\mathcal{F}$	rat14	0.00167	1	0.04087
$\mathcal{AZI}$	rat14	0.0004311	1.000	0.02076
$\mathcal{J}$	rat13	0.00561	1.000	0.05296
$\mathcal{R}e\mathcal{G}_1$	rat13	0.002809	1	0.03748
$\mathcal{R}e\mathcal{G}_2$	rat21	0.01276	1	0.06521
$\mathcal{R}e\mathcal{G}_3$	rat23	0.000422	1	0.02054

3.1.5 *Entropy* vs Indices

Graphical models of entropy vs indices are shown in figures 28-44.

$$Entropy(\mathcal{R}_1) = \frac{p_1 \times (\mathcal{R}_1) + p_2}{(\mathcal{R}_1)^2 + q_1 \times (\mathcal{R}_1) + q_2},$$

where $(\mathcal{R}_1)$ is normalized by mean 7040 and std 6110.

Parametric values (alongside 95% $\mathcal{CI}$):

$p_1 = 2e + 04$, $(\mathcal{R}\_1) = (561, 4e + 04)$

$p_2 = 2.529e + 04$, $\mathcal{CI} = (710, 5e + 04)$

$q_1 = -3.7$, $\mathcal{CI} = (-5.6, -1.9)$

$q_2 = 248$, $\mathcal{CI} = (7, 489)$

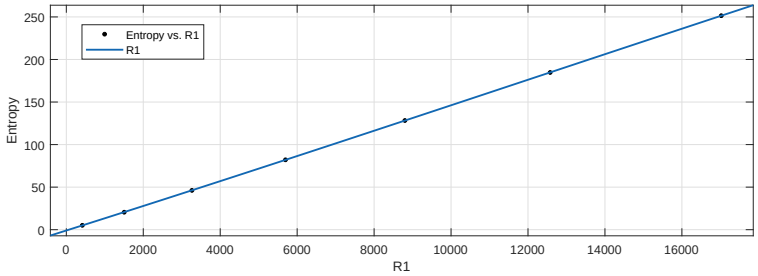

Figure 28: *Entropy* vs $\mathcal{R}_1$

$$Entropy(\mathcal{R}_{-1}) = \frac{p_1 \times (\mathcal{R}_{-1})^2 + p_2 \times (\mathcal{R}_{-1}) + p_3}{(\mathcal{R}_{-1})^2 + q_1 \times (\mathcal{R}_{-1}) + q_2},$$

where $(\mathcal{R}\_1)$ is normalized by mean 86 and std 77.46.

Parametric values (alongside 95% $\mathcal{CI}$):

$p_1 = 4.795e + 04$, $\mathcal{CI}= (2e + 04, 7.718e + 04)$

$p_2 = e + 05$, $\mathcal{CI}= (4e + 04, 2e + 05)$

p_3=$7.612e + 04$, $\mathcal{CI}$=$(2e + 04, e + 05)$ $q_1 = 532$, $\mathcal{CI}= (206, 858)$

$q_2 = 738$, $\mathcal{CI}= (220, 1255)$

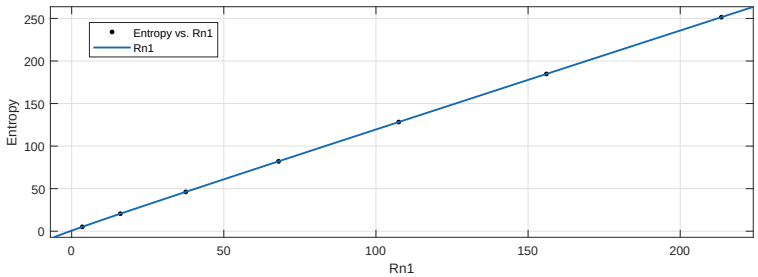

Figure 29: *Entropy* vs $\mathcal{R}_{-1}$

$$Entropy(\mathcal{R}_{\frac{1}{2}}) = \frac{p_1 \times (\mathcal{R}_{\frac{1}{2}})^2 + p_2 \times (\mathcal{R}_{\frac{1}{2}}) + p_3}{(\mathcal{R}_{\frac{1}{2}})^2 + q_1 \times (\mathcal{R}_{\frac{1}{2}}) + q_2},$$

where $(\mathcal{R}_{\frac{1}{2}})$ is normalized by mean 86 and std 77.46.

Parametric values (alongside 95% $\mathcal{CI}$):

$p_1 = e + 06$, $\mathcal{CI}= (-9e + 07, 9e + 07)$

$p_2 = 3e + 06$, $\mathcal{CI}= (-2e + 08, 2e + 08)$

p_3=$2e + 06$, $\mathcal{CI}$=$(-e + 08, e + 08)$ $q_1 = e + 04$, $\mathcal{CI}= (-e + 06, e + 06)$

$q_2 = 2e + 04$, $\mathcal{CI}= (-e + 06, 2e + 06)$

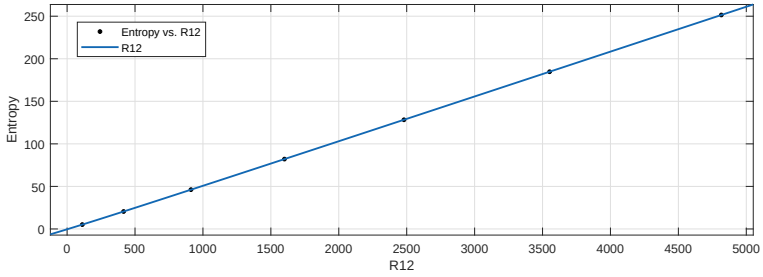

Figure 30: *Entropy* vs $\mathcal{R}_{\frac{1}{2}}$

$$Entropy(\mathcal{R}_{-\frac{1}{2}}) = \frac{p_1 \times (\mathcal{R}_{-\frac{1}{2}}) + p_2}{(\mathcal{R}_{-\frac{1}{2}})^4 + q_1 \times (\mathcal{R}_{-\frac{1}{2}})^3 + q_2 \times (\mathcal{R}_{-\frac{1}{2}})^2 + q_3 \times (\mathcal{R}_{-\frac{1}{2}}) + q_4},$$

where $(\mathcal{R}_{-\frac{1}{2}})$ is normalized by mean 222.6 and std 198.8.

Parametric values (alongside 95% $\mathcal{CI}$):

$p1 = -4e+04$, $\mathcal{CI}= (-3e+05, 2e+05)$

$p_2 = -5.175e+04$, $\mathcal{CI}= (-3e+05, 2e+05)$

$q_1 = -3$, $\mathcal{CI}= (-9, 3)$

$q_2 = 3$, $\mathcal{CI}= (-15.1, 21.94)$

$q_3 = -4$, $\mathcal{CI}= (-31, 24)$

$q_4 = -503$, $\mathcal{CI}= (-3384, 2379)$

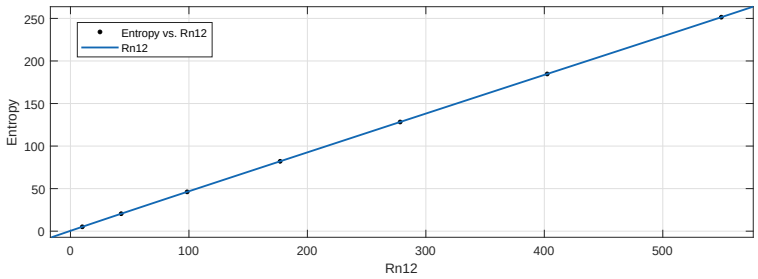

Figure 31: *Entropy* vs $\mathcal{R}_{-\frac{1}{2}}$

$$Entropy(\mathcal{ABC}) = \frac{(p_1 \times (\mathcal{ABC})^2 + p_2 \times (\mathcal{ABC}) + p_3}{(\mathcal{ABC})^2 + q_1 \times (\mathcal{ABC}) + q_2},$$

where $(\mathcal{ABC})$ is normalized by mean 454.8 and std 404.1.

Parametric values (alongside 95% $\mathcal{CI}$):

$p_1 = -e+06$, $\mathcal{CI}= (-5e+07, 5e+07)$

$p_2 = -4e+06$, $\mathcal{CI}= (-e+08, e+08)$ $p_3 = -2.766e+06$, $\mathcal{CI}= (-10e+07, 9e+07)$

$q_1 = -e+04$, $\mathcal{CI}= (-6e+05, 5e+05)$

$q_2 = -2e+04$, $\mathcal{CI}= (-9e+05, 9e+05)$

$$Entropy(\mathcal{GA}) = \frac{p_1 \times (\mathcal{GA}) + p_2}{(\mathcal{GA})^4 + q_1 \times (\mathcal{GA})^3 + q_2 \times (\mathcal{GA})^2 + q_3 + q_4},$$

where $(\mathcal{GA})$ normalized by mean 591.5 and std 521.5.

Parametric values (alongside 95% $\mathcal{CI}$):

$p_1 = 1.692e+05$, $\mathcal{CI}= (-8e+05, e+06)$

$p_2 = 1.917e+05$, $\mathcal{CI}= (-9e+05, e+06)$

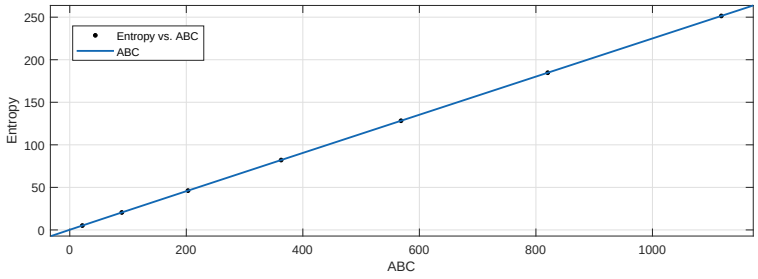

Figure 32: *Entropy* vs $\mathcal{ABC}$

$q_1 = -3.01$, $\mathcal{CI}$=$(-8, 3)$

$q_2 = 3$, $\mathcal{CI}$= $(-15, 22)$ $q_3 = -4$, $\mathcal{CI}$= $(-33, 24)$

$q_4 = 1869$, $\mathcal{CI}$= $(-8823, e + 04)$

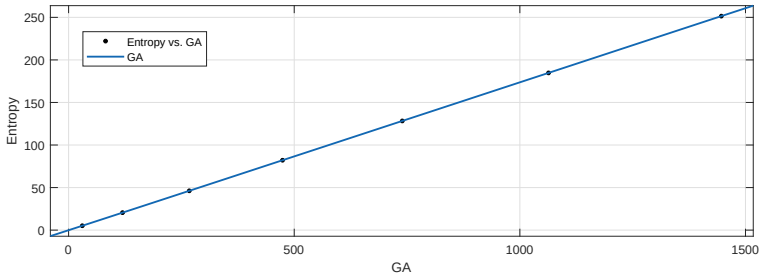

Figure 33: *Entropy* vs $\mathcal{GA}$

$$Entropy(\mathcal{M}_1) = \frac{p_1 \times (\mathcal{M}_1)^2 + p_2 \times (\mathcal{M}_1) + p_3}{(\mathcal{M}_1)^2 + q_1 \times (\mathcal{M}_1) + q_2},$$

where $(\mathcal{M}_1)$ is normalized by mean 4320 and std 3791.

Parametric values (alongside 95% $\mathcal{CI}$):

$p1 = 5e + 06$, $\mathcal{CI}$= $(-e + 09, 2e + 09)$

$p_2 = 1.266e + 07$, $\mathcal{CI}$= $(-4e + 09, 4e + 09)$

$p_3 = 7.81e + 06$, $\mathcal{CI}$= $(-2e + 09, 3e + 09)$

$q_1 = 5.598e + 04$, $\mathcal{CI}$= $(-2e + 07, 2e + 07)$ $q_2 = 7.624e + 04$, $\mathcal{CI}$= $(-2e + 07, 2e + 07)$

$$Entropy(\mathcal{M}_2) = \frac{p_1 \times (\mathcal{M}_2) + p_2}{(\mathcal{M}_2)^4 + q_1 \times (\mathcal{M}_2)^3 + q_2 \times (\mathcal{M}_2)^2 + q_3 \times (\mathcal{M}_2) + q_4},$$

where $(\mathcal{M}_2)$ is normalized by mean 4224 and std 3712.

Parametric values (alongside 95% $\mathcal{CI}$):

$p1 = 7.805e + 04$, $\mathcal{CI}$= $(-3e + 05, 5e + 05)$

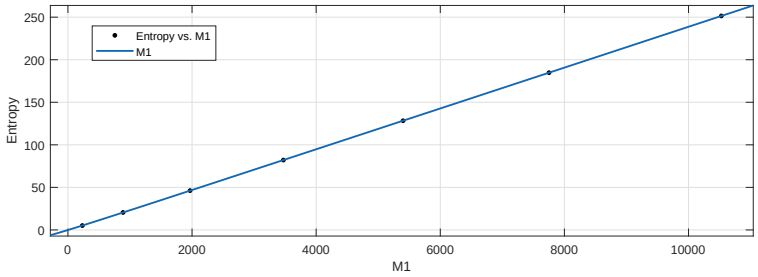

Figure 34: *Entropy* vs $\mathcal{M}_1$

$p_2 = 9e+04$, $\mathcal{CI}= (-4e+05, 6e+05)$

$q_1 = -3$, $\mathcal{CI}= (-9, 3)$

$q_2 = 3.521$, $\mathcal{CI}= (-15, 22)$

$q_3 = -4$, $\mathcal{CI}= (-33, 24)$

$q_4 = 865$, $\mathcal{CI} = (-4065, 5795)$

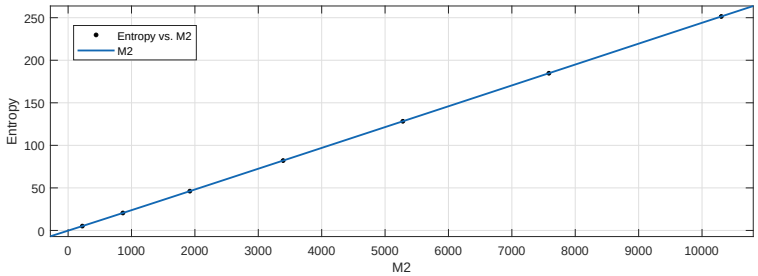

Figure 35: *Entropy* vs $\mathcal{M}_2$

$$Entropy(\overline{\mathcal{M}_1}) = \frac{p_1 \times (\overline{\mathcal{M}_1})^2 + p_2 \times (\overline{\mathcal{M}_1}) + p_3}{(\overline{\mathcal{M}_1})^2 + q_1 \times (\overline{\mathcal{M}_1}) + q_2},$$

where $(\overline{\mathcal{M}_1})$ is normalized by mean $1.026e+07$ and std $1.372e+07$.

Parametric values (alongside 95% $\mathcal{CI}$):

$p_1 = 523$, $\mathcal{CI} = (300, 745)$

$p_2 = 1032$, $\mathcal{CI}= (309, 1754)$

$p_3 = 480$, $\mathcal{CI}= (58, 902)$

$q_1 = 5$, $\mathcal{CI}= (2, 9)$

$q_2 = 3$, $\mathcal{CI}= (0.4, 7)$

$$Entropy(\overline{\mathcal{M}_2}) = \frac{p_1 \times (\overline{\mathcal{M}_2})^2 + p_2 \times (\overline{\mathcal{M}_2}) + p_3}{(\overline{\mathcal{M}_2})^2 + q_1 \times (\overline{\mathcal{M}_2}) + q_2},$$

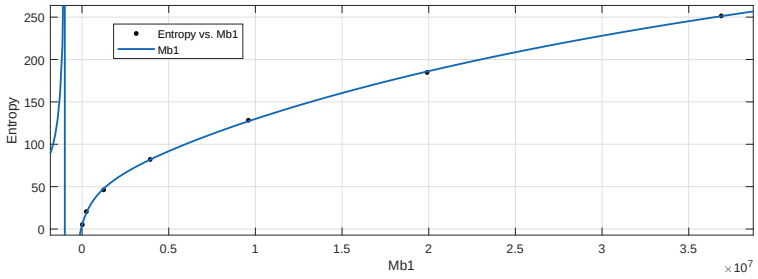

Figure 36: *Entropy* vs $\overline{\mathcal{M}_1}$

where $(\overline{\mathcal{M}_2})$ is normalized by mean $7.632e+05$ and std $1.023e+06$

Parametric values (alongside 95% $\mathcal{CI}$):

$p_1 = -1e+06$, $\mathcal{CI}$= $(-7e+10, 7e+10)$

$p_2 = -8e+06$, $\mathcal{CI}$= $(-3e+11, 3e+11)$

$p_3 = -5e+06$, $\mathcal{CI}$= $(-2e+11, 2e+11)$

$q_1 = -3e+04$, $\mathcal{CI}$= $(-1e+09, 1e+09)$

$q_2 = -3e+04$, $\mathcal{CI}$= $(-1e+09, 1e+09)$

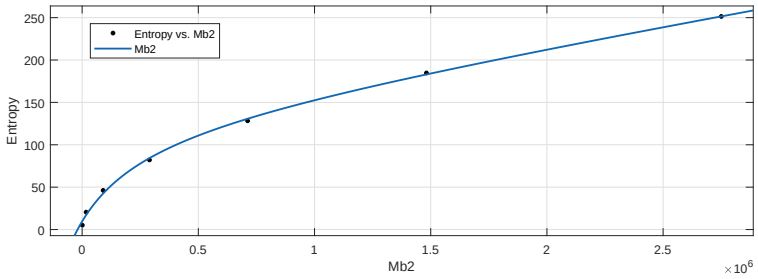

Figure 37: *Entropy* vs $\overline{\mathcal{M}_2}$

$$Entropy(\mathcal{HM}) = \frac{p_1 \times (\mathcal{HM})^2 + p_2 \times (\mathcal{HM}) + p_3}{(\mathcal{HM})^2 + q_1 \times (\mathcal{HM}) + q_2},$$

where $(\mathcal{HM})$ is normalized by mean $9.802e+04$ and std $8.409e+04$

Parametric values (alongside 95% $\mathcal{CI}$):

$p_1 = -3e+04$, $\mathcal{CI} = (-5e+04, -1e+04)$

$p_2 = -8e+04$, $\mathcal{CI}$= $(-1e+05, -3e+04)$

$p_3 = -5e+04$, $\mathcal{CI} = (-8e+04, -1e+04)$

$q_1 = -341$, $\mathcal{CI}$= $(-538, -144)$

$q_2 = -517$, $\mathcal{CI}$= $(-862, -172)$

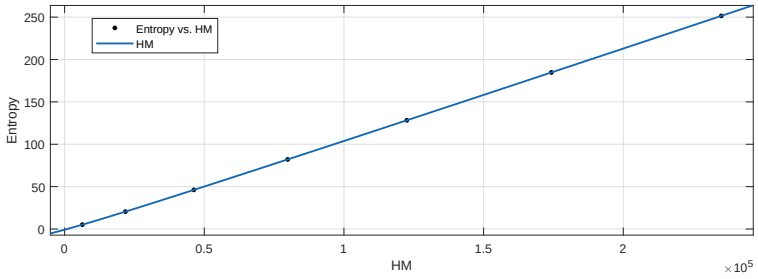

Figure 38: *Entropy* vs $\mathcal{HM}$

$$Entropy(\mathcal{F}) = \frac{p_1 \times (\mathcal{F}) + p_2}{(\mathcal{F})^4 + q_1 \times (\mathcal{F})^3 + q_2 \times (\mathcal{F})^2 + q_3 \times (\mathcal{F}) + q_4},$$

where $(\mathcal{F})$ is normalized by mean $1.635e+04$ and std $1.43e+04$

Parametric values (alongside 95% $\mathcal{CI}$):

$p_1 = -5e+06$, $\mathcal{CI}= (-9e+09, 9e+09)$

$p_2= -6e+06$, $\mathcal{CI}= (-1e+10, 1e+10)$

$q_1= 123$, $\mathcal{CI}= (-2e+05, 2e+05)$

$q_2 = -410$, $\mathcal{CI}= (-7e+05, 7e+05)$

$q_3 = 626$, $\mathcal{CI}= (-1e+06, 1e+06)$

$q_4 = -6e+04$, $\mathcal{CI}= (-1e+08, 1e+08)$

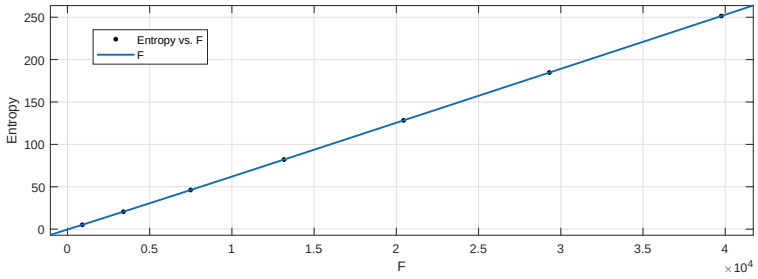

Figure 39: *Entropy* vs $\mathcal{F}$

$$Entropy(\mathcal{AZI}) = \frac{p_1 \times (\mathcal{AZI}) + p_2}{(\mathcal{AZI})^2 + q_1 \times (\mathcal{AZI}) + q_2},$$

where $(\mathcal{AZI})$ is normalized by mean 7718 and std 6667

Parametric values (alongside 95% $\mathcal{CI}$):

$p_1 = 1e+04$, $\mathcal{CI}= (519, 3e+04)$

$p_2 = 2e+04$, $\mathcal{CI}= (663, 4e+04)$

$q_1 = -3$, $\mathcal{C}I= (-5, -2)$

$q_2 = 197$, $\mathcal{CI}= (6, 387)$

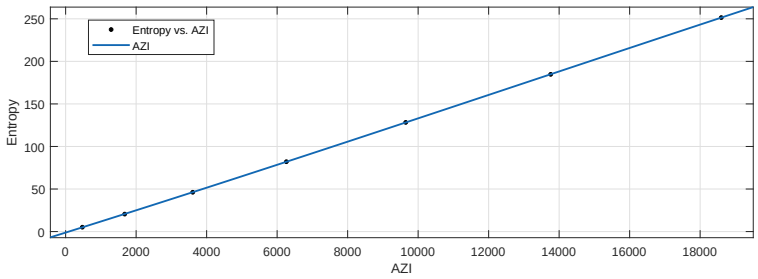

Figure 40: *Entropy* vs $\mathcal{AZI}$

$$Entropy(\mathcal{J}) = \frac{p_1 \times (\mathcal{J})^2 + p_2 \times (\mathcal{J}) + p_3}{(\mathcal{J})^2 + q_1 \times (\mathcal{J}) + q_2},$$

where $(\mathcal{J})$ is normalized by mean 494.8 and std 437.4.

Parametric values (alongside 95% $\mathcal{CI}$):

$p_1 = -2e + 06$, $(-3e + 08, 3e + 08)$

$p_2 = -6e + 06$, $(-7e + 08, 7e + 08)$

$p_3 = -4e + 06$, $(-4e + 08, 5e + 08)$

$q_1 = -2e + 04$, $(-3e + 06, 3e + 06)$

$q_2 = -4e + 04$, $(-5e + 06, 4e + 06)$

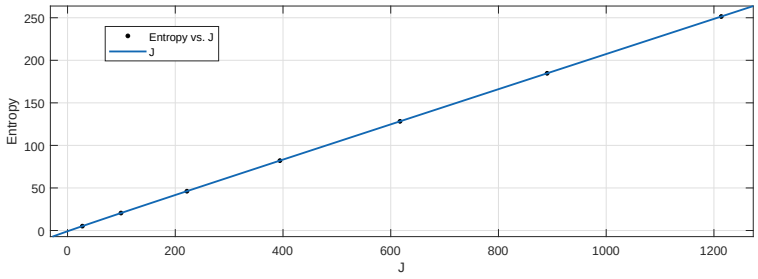

Figure 41: *Entropy* vs $\mathcal{J}$

$$Entropy(\mathcal{ReZG}_1) = \frac{p_1 \times (\mathcal{ReZG}_1)^2 + p_2 \times (\mathcal{ReZG}_1) + p_3}{(\mathcal{ReZG}_1)^3 + q_1 \times (\mathcal{ReZG}_1)^2 + q_2 \times (\mathcal{ReZG}_1) + q_3},$$

where $(\mathcal{ReZG}_1)$ is normalized by mean 504 and std 451.3

Parametric values (alongside 95% $\mathcal{CI}$):

$p_1 = 2e + 06$, $\mathcal{CI}= (-3e + 09, 3e + 09)$

$p_2 = 7e + 06$, $\mathcal{CI}=(-8e + 09, 8e + 09)$

$p_3 = 5e+06$, $\mathcal{CI}$=$(-5e+09, 5e+09)$

$q_1 = -0.7$, $\mathcal{CI}$= $(-2721, 2720)$

$q_2 = 2e+04$, $\mathcal{CI}$= $(-3e+07, 3e+07)$

$q_3 = 4e+04$, $\mathcal{CI}$= $(-5e+07, 5e+07)$

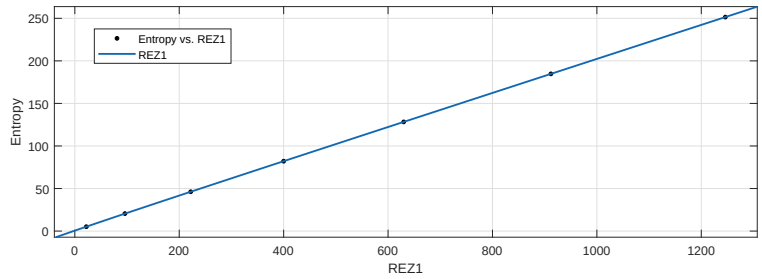

Figure 42: *Entropy* vs $\mathcal{ReZG}_1$

$$Entropy(\mathcal{ReZG}_2) = \frac{p_1 \times (\mathcal{ReZG}_2)^2 + p_2 \times (\mathcal{ReZG}_2) + p_3}{(\mathcal{ReZG}_2)^3 + q_1 \times (\mathcal{ReZG}_2)^2 + q_2 \times (\mathcal{ReZG}_2) + q_3},$$

where $\mathcal{ReZG}_2$)is normalized by mean 968.5 and std 845.7.

Parametric values (alongside 95% $\mathcal{CI}$):

$p_1 = -3e+06$, $\mathcal{CI}$= $(-1e+09, 1e+09)$

$p_2 = -9e+06$, $\mathcal{CI}$=$(-3e+09, 3e+09)$

$p_3 = -6e+06$, $\mathcal{CI}$=$(-2e+09, 2e+09)$

$q_1 = 39$, $\mathcal{CI}$=$(-1e+04, 1e+04)$

$q_2 = -4e+04$, $\mathcal{CI}$=$(-1e+07, 1e+07)$

$q_3 = -6e+04$, $\mathcal{CI}$=$(-2e+07, 2e+07)$

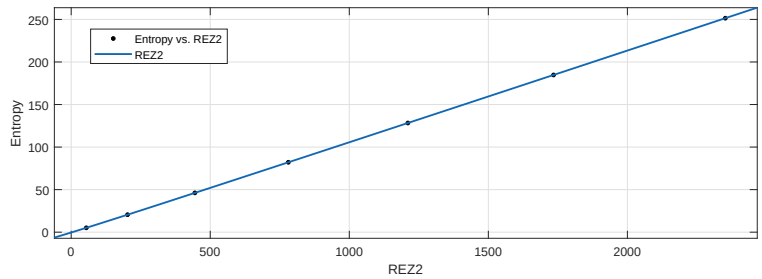

Figure 43: *Entropy* vs $\mathcal{ReZG}_2$

$$Entropy(\mathcal{ReZG}_3) = \frac{p_1 \times (\mathcal{ReZG}_3) + p_2}{(\mathcal{ReZG}_3)^4 + q_1 \times (\mathcal{ReZG}_3)^3 + q_2 \times (\mathcal{ReZG}_3)^2 + q_3 \times (\mathcal{ReZG}_3) + q_4},$$

where ($\mathcal{R}e\mathcal{Z}\mathcal{G}_3$) is normalized by mean $5e+04$ and std $4e+04$.

Parametric values (alongside 95% $\mathcal{CI}$):

$p_1 = 2e+04$, $\mathcal{CI}$=$(-9e+04, 1e+05)$

$p_2 = 2e+04$, $\mathcal{CI}$=$(-1e+05, 1e+05)$

$q_1 = -3$, $\mathcal{CI}$=$(-8, 3)$

$q_2 = 3$, $\mathcal{CI}$=$(-15, 22)$

$q_3 = -4$, $\mathcal{CI}$=$(-34, 25)$

$p_4 = 235.1$, $\mathcal{CI}$=$(-1079, 1549)$

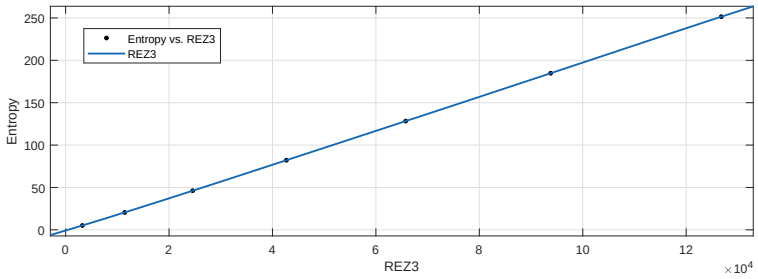

Figure 44: *Entropy* vs $\mathcal{R}e\mathcal{Z}\mathcal{G}_3$

Table 11: Entropy Goodness of Fit versus IndicesTbO_2.

Index	Fit Type	$\mathcal{SSE}$	$\mathcal{R}^2$	$\mathcal{RMSE}$
$\mathcal{R}_1$	rat12	0.06044	1	0.1419
$\mathcal{R}_{-1}$	rat22	0.0002752	1	0.01173
$\mathcal{R}_{\frac{1}{2}}$	rat22	0.00489	1	0.04945
$\mathcal{R}_{-\frac{1}{2}}$	rat14	0.0008022	1	0.02832
$\mathcal{ABC}$	rat22	0.000446	1	0.01493
$\mathcal{GA}$	rat14	5.669e-05	1	0.007529
$\mathcal{M}_1$	rat22	0.00934	1	0.06834
$\mathcal{M}_2$	rat14	0.0002615	1	0.01617
$\overline{\mathcal{M}_1}$	rat22	7.605	0.9998	1.95
$\overline{\mathcal{M}_2}$	rat22	62.19	0.9987	5.576
$\mathcal{HM}$	rat22	0.0004494	1.000	0.01499
$\mathcal{F}$	rat14	0.0005799	1.000	0.07615
$\mathcal{AZI}$	rat12	0.09443	1.000	0.1774
$\mathcal{J}$	rat22	0.003381	1.000	0.04111
$\mathcal{R}e\mathcal{G}_1$	rat23	0.002288	1.000	0.04784
$\mathcal{R}e\mathcal{G}_2$	rat23	0.000187	1.000	0.01367
$\mathcal{R}e\mathcal{G}_3$	rat14	0.003319	1.000	0.05761

3.2 Graphite Carbon Nitride Results

3.2.1 Topological Indices of $g - C_3N_4$

Order and size of the chemical graph of polycyclic graphite carbon nitride structure, denoted as $g - C_3N_4$, are $14lk + l + k$ and $18lk$, respectively. Because there are three different types of vertices in $g - C_3N_4$ specifically, the vertices of degree 1, 2, 3, respectively. Vertex partition of the vertex set $g - C_3N_4$ is shown in table 12. Edge partition of $g - C_3N_4$ based on the degrees of each edge's end vertices are displayed in table 13.

Table 12: Partitioning of set of vertices of $g - C_3N_4$

$\widetilde{\Im}(s)$	Frequency	Vertex Set
1	$l + k + 1$	$\mathcal{V}_1$
2	$6lk + l + k - 2$	$\mathcal{V}_2$
3	$8lk - l - k + 1$	$\mathcal{V}_3$

Table 13: Partitioning of set of edges of $g - C_3N_4$

$(\widetilde{\Im}(s),\ \widetilde{\Im}(t))$	Frequency	Set of Edges
$(1, 3)$	$l + k + 1$	$\mathcal{E}_1$
$(2, 3)$	$12lk + 2l + 2k - 4$	$\mathcal{E}_2$
$(3, 3)$	$6lk - 3l - 3k + 3$	$\mathcal{E}_3$

Let $\mathcal{G}$ denote the chemical graph of $g - C_3N_4$ and $\widetilde{\Im}(s)$ represent the degree of vertex s.

- $\mathcal{GR}$ index of $g - C_3N_4$

For $\alpha = 1$,

$$\begin{aligned}
\mathcal{R}_1(\mathcal{G}) &= \sum_{st \in \mathcal{E}(\mathcal{G})} (\widetilde{\Im}(s) \times \widetilde{\Im}(t)) \\
&= (l + k + 1)(1 \times 3) + (12lk + 2l + 2k - 4)(2 \times 3) + (6lk - 3l - 3k + 3)(3 \times 3) \\
&= 126lk - 12l - 12k
\end{aligned}$$

For $\alpha = -1$,

$$\begin{aligned}
\mathcal{R}_{-1}(\mathcal{G}) &= \sum_{st\in\mathcal{E}(\mathcal{G})} \frac{1}{(\widetilde{\Im}(s)\times\widetilde{\Im}(t))} \\
&= (l+k+1)\frac{1}{(1\times 3)} + (12lk+2l+2k-4)\frac{1}{(2\times 3)} + (6lk-3l-3k+3)\frac{1}{(3\times 3)} \\
&= \frac{8}{3}lk + \frac{1}{3}l + \frac{1}{3}k.
\end{aligned}$$

For $\alpha = \frac{1}{2}$,

$$\begin{aligned}
\mathcal{R}_{\frac{1}{2}}(\mathcal{G}) &= \sum_{st\in\mathcal{E}(\mathcal{G})} \sqrt{(\widetilde{\Im}(s)\times\widetilde{\Im}(t))} \\
&= (l+k+1)\sqrt{(1\times 3)} + (12lk+2l+2k-4)\sqrt{(2\times 3)} \\
&+ (6lk-3l-3k+3)\sqrt{(3\times 3)} \\
&= 47.393877lk - 2.36897l - 2.36897k + 0.934092.
\end{aligned}$$

For $\alpha = -\frac{1}{2}$,

$$\begin{aligned}
\mathcal{R}_{-\frac{1}{2}}(\mathcal{G}) &= \sum_{st\in\mathcal{E}(\mathcal{G})} \frac{1}{\sqrt{(\widetilde{\Im}(s)\times\widetilde{\Im}(t))}} \\
&= (l+k+1)\frac{1}{\sqrt{(1\times 3)}} + (12lk+2k+2l-4)\frac{1}{\sqrt{(2\times 3)}} \\
&+ (6lk-3l-3k+3)\frac{1}{\sqrt{(3\times 3)}} \\
&= 6.898979lk + 0.393847l + 0.393847k - 0.055643.
\end{aligned}$$

The numerical representation of the above-mentioned computed results is shown in table 14.

Table 14: Randic index for $\alpha = 1, -1, \frac{1}{2}, -\frac{1}{2}$

$[\boldsymbol{l}, \boldsymbol{k}]$	$\mathcal{R}_1(\mathcal{G})$	$\mathcal{R}_{-1}(\mathcal{G})$	$\mathcal{R}_{\frac{1}{2}}(\mathcal{G})$	$\mathcal{R}_{-\frac{1}{2}}(\mathcal{G})$
$[1,1]$	108	3.33	43.59	7.63
$[2,2]$	462	12	181.03	29.12
$[3,3]$	1068	26	413.27	64.40
$[4,4]$	1926	45.33	740.28	113.48
$[5,5]$	3036	70	1162.09	176.36
$[6,6]$	4398	100	1678.68	253.03
$[7,7]$	6012	135.33	2290.07	343.51

- $\mathcal{ABC}$ index of $g - C_3N_4$

$$\begin{aligned}
\mathcal{ABC}(\mathcal{G}) &= \sum_{st\in\mathcal{E}(\mathcal{G})}\sqrt{\frac{\widetilde{\Im}(s)+\widetilde{\Im}(t)-2}{d_s d_t}} \\
&= (l+k+1)\sqrt{\frac{1+3-2}{1\times 3}}+(12lk+2l+2k-4)\sqrt{\frac{2+3-2}{2\times 3}} \\
&+ (6lk-3l-3k+3)\sqrt{\frac{3+3-2}{3\times 3}} \\
&= \sqrt{\frac{2}{3}}\,(l+k+1)+\sqrt{\frac{1}{2}}\,(12lk+2l+2k-4)+2\,(2lk-l+1-k) \\
&= 12.4853lk+0.2307l+0.2307k-0.0119.
\end{aligned}$$

- $\mathcal{GA}$ index of $g - C_3N_4$

$$\begin{aligned}
\mathcal{GA}(\mathcal{G}) &= \sum_{st\in\mathcal{E}(G)}\frac{2\sqrt{\widetilde{\Im}(s)\times\widetilde{\Im}(t)}}{\widetilde{\Im}(s)+\widetilde{\Im}(t)} \\
&= (l+k+1)\frac{2\sqrt{1\times 3}}{1+3}+(12lk+2l+2k-4)\frac{2\sqrt{2\times 3}}{2+3} \\
&+ (6lk-3l-3k+3)\frac{2\sqrt{3\times 3}}{3+3} \\
&= \frac{\sqrt{3}\,(l+k+1)}{2}+\frac{24\sqrt{6}lk+4\sqrt{6}l+4\sqrt{6}k-8\sqrt{6}}{5}+6lk-3l+3-3k \\
&= 17.757551lk-0.174383l-0.174383k-0.054158.
\end{aligned}$$

The numerical representation of the above-mentioned computed results is shown in table 15.

Table 15: $\mathcal{ABC}$ and $\mathcal{GA}$ indices for $g - C_3N_4$.

$[\boldsymbol{l},\boldsymbol{k}]$	$\mathcal{ABC}(\mathcal{G})$	$\mathcal{GA}(\mathcal{G})$
$[1,1]$	12.92	17.36
$[2,2]$	50.85	70.28
$[3,3]$	113.74	158.72
$[4,4]$	201.60	282.67
$[5,5]$	314.43	442.14
$[6,6]$	452.23	637.12
$[7,7]$	614.99	867.63

- $\mathcal{M}_1$ and $\mathcal{M}_2$ indices of $g - C_3N_4$

$$\begin{aligned}\mathcal{M}_1(\mathcal{G}) &= \sum_{st\in\mathcal{E}(\mathcal{G})}(\widetilde{\Im}(s)+\widetilde{\Im}(t))\\ &= (l+k+1)(1+3)+(12lk+2l+2k-4)(2+3)+(6lk-3l-3k+3)(3+3)\\ &= 96lk-4l-4k+2.\end{aligned}$$

$$\begin{aligned}\mathcal{M}_2(\mathcal{G}) &= \sum_{st\in\mathcal{E}(\mathcal{G})}(\widetilde{\Im}(s)\times\widetilde{\Im}(t))\\ &= (l+k+1)(1\times 3)+(12lk+2l+2k-4)(2\times 3)\\ &+ (6lk-3l-3k+3)(3\times 3)\\ &= 126lk-12l-12k+6.\end{aligned}$$

- $\overline{\mathcal{M}_1}$ and $\overline{\mathcal{M}_2}$ of $g-C_3N_4$

$$\begin{aligned}\overline{\mathcal{M}_1}(\mathcal{G}) &= \sum_{pq\notin\mathcal{E}(\mathcal{G})}(\widetilde{\Im}(s)+\widetilde{\Im}(t))\\ &= 2(18lk)(14lk+l+k-1)-(96lk-4l-4k+2)\\ &= 504l^2k^2+36l^2k+36lk^2-132lk+4l+4k-2.\end{aligned}$$

$$\begin{aligned}\overline{\mathcal{M}_2}(\mathcal{G}) &= \sum_{pq\notin\mathcal{E}(\mathcal{G})}(\widetilde{\Im}(s)\times\widetilde{\Im}(t))\\ \overline{\mathcal{M}_2}(\mathcal{G}) &= 2(18lk)^2-\frac{1}{2}(96lk-4l-4k+2)-(126lk-12l-12k+6)\\ &= 648l^2k^2+14l-174lk+14k-7.\end{aligned}$$

The numerical representation of the above-mentioned computed results is shown in Table 16.

Table 16: Consideration of $\mathcal{M}_1(\mathcal{G})$, $\mathcal{M}_2(\mathcal{G})$, $\overline{\mathcal{M}_1}(\mathcal{G})$, $\overline{\mathcal{M}_2}(\mathcal{G})$ indices for $g-C_3N_4$.

$[\boldsymbol{k},\boldsymbol{l}]$	$\mathcal{M}_1(\mathcal{G})$	$\mathcal{M}_2(\mathcal{G})$	$\overline{\mathcal{M}_1}(\mathcal{G})$	$\overline{\mathcal{M}_2}(\mathcal{G})$
$[1,1]$	90	108	450	495
$[2,2]$	370	462	8126	9721
$[3,3]$	842	1068	41602	50999
$[4,4]$	1506	1926	131550	163209
$[5,5]$	2362	3036	320738	400783
$[6,6]$	3410	4398	664030	833705
$[7,7]$	4650	6012	1228386	1547511

3.2.2 Entropy and Heat of Formation $g - C_3N_4$

Figure 45 depicts the synthesis reaction path of $g - C_3N_4$ from the precursors of urea and dicyanodiamine. $g - C_3N_4$ has a standard molar enthalpy of $18.70 kJmol^{-1} (4.47 kcal/mol)$. The

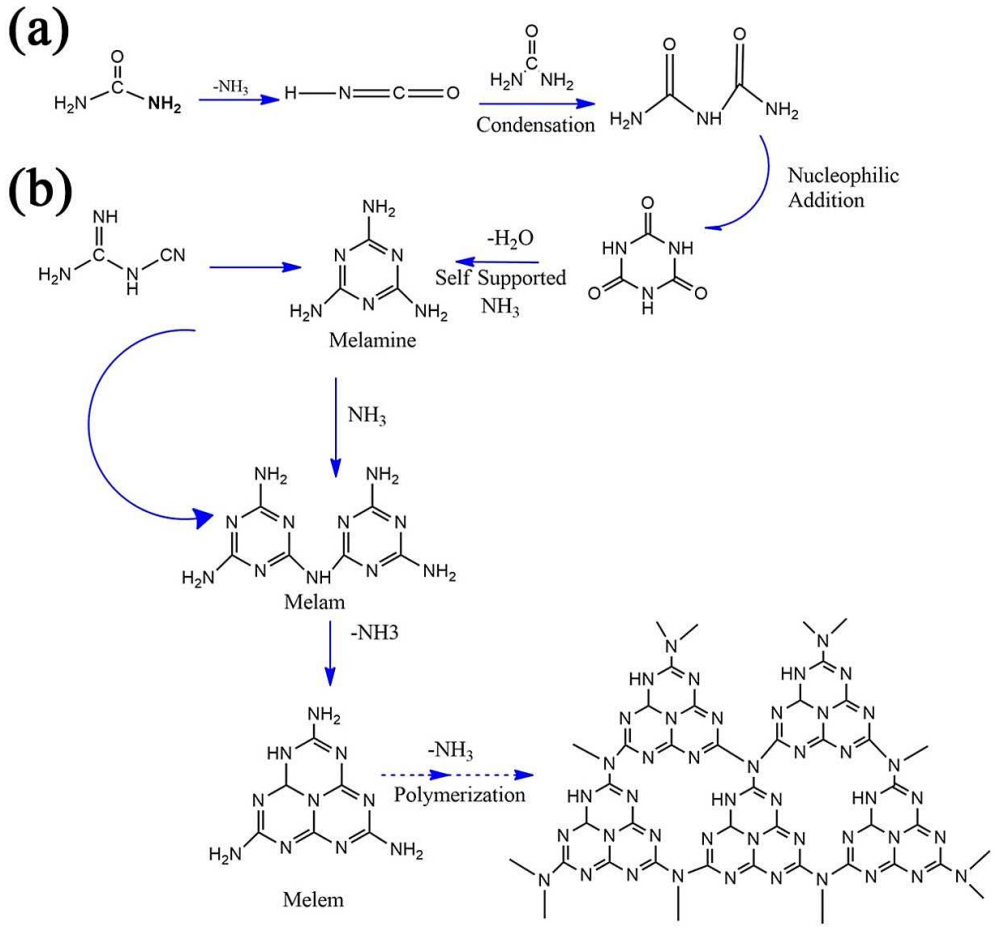

Figure 45: Synthesis of Graphitic Carbon Nitride from (a) Dicyanodiamine Precursors and (b)Urea [36].

enthalpy of $g - C_3N_4$ has an inverse relationship with its crystal size, decreasing as the number of unit cells increases, according to these calculations. The entropy of $g - C_3N_4$ was calculated using the same approach. $g - C_3N_4$ has a molar standard entropy of $77 Jmol^{-1}K^{-1}$. For each formula unit, Avogadro's number was divided by the molar standard entropy. The result was then multiplied by the number of formula units found in a single unit cell.

Entropy and $\mathcal{H}o\mathcal{F}$ parameters for various values of l and k are given in table 17. Figure 46-48

Table 17: $\mathcal{H}o\mathcal{F}$ and entropy values for $g - C_3N_4$

$[l, k]$	Formula Units	Entropy $\times 10^{22} kJ$	Heat of Formation $\times 10^{22} kJ$
$[1, 1]$	4	5.117	1.242
$[2, 2]$	16	0.204	4.968
$[3, 3]$	36	0.460	0.111
$[4, 4]$	64	0.818	0.198
$[5, 5]$	100	0.012	0.310
$[6, 6]$	144	0.018	0.447
$[7, 7]$	196	0.025	0.608

show the comparisons.

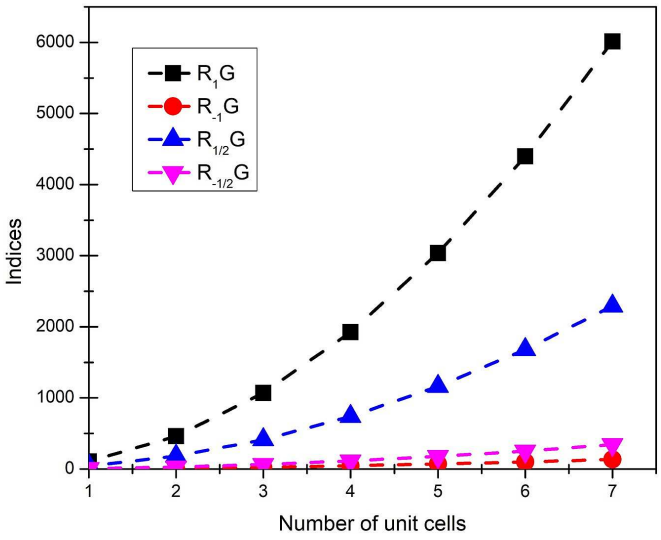

Figure 46: Graphical Representations of $\mathcal{R}_1$, $\mathcal{R}_{-1}$, $\mathcal{R}_{1/2}$ and $\mathcal{R}_{-1/2}$

3.2.3 $\mathcal{H}o\mathcal{F}$(and Entropy) and Indices Curve Fitting

We can study the link between several variables is a set of data. This analysis was performed to investigate the relationship between formation heat/entropy and several variables. Several curve fitting approaches are employed to obtain a graphical model for ($\mathcal{H}o\mathcal{F}$) and entropy vs several degree based indices.

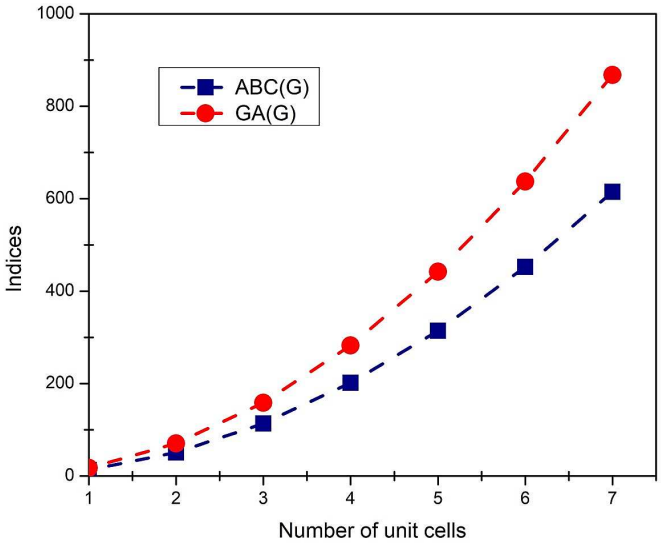

Figure 47: Graphical Representations of $\mathcal{ABC}$, $\mathcal{GA}$

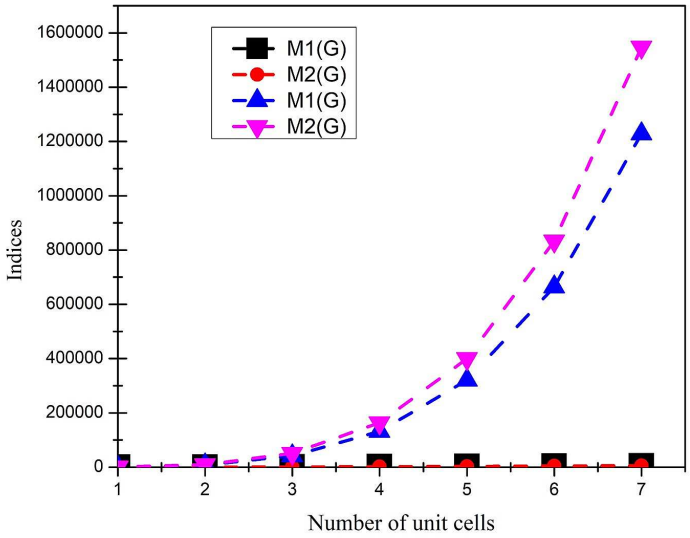

Figure 48: Graphical Representations of $\mathcal{M}_1$, $\mathcal{M}_2$, $\overline{\mathcal{M}_1}$ and $\overline{\mathcal{M}_2}$

3.2.4 General models for Indices vs $\mathcal{HoF}$

Graphical models of HoF vs indices are shown figures 49, 50, 51, 52 and 53. Parametric for each graphical fitted model are provided along with 95% $\mathcal{CI}$ in the following computations.

$$\mathcal{HoF}(\mathcal{R}_1) = \frac{p_1 \times \mathcal{R}_1^3 + p_2 \times \mathcal{R}_1^2 + p_3 \times \mathcal{R}_1 + p_4}{\mathcal{R}_1^2 + q_1 \times \mathcal{R}_1 + q_2} \tag{5}$$

Parametric values (alongside 95% $\mathcal{CI}$):

$p_1 = 1e{-}05(-0.005, 0.005)$, $p_2 = 0.5(-1051, 1052)$, $p_3 = -547(-5e{+}07, 5e{+}07)$, $p_4 = 18(-6e{+}10, 6e + 10)$, $q_1 = -525(-1e + 08, 1e + 08)$, $q_2 = 26(-5e + 10, 5e + 10)$.

$$\mathcal{HoF}(\mathcal{R}_{-1}) = \frac{p_1 \times \mathcal{R}_{-1}^2 + p_2 \times \mathcal{R}_{-1} + p_3}{\mathcal{R}_{-1} + q_1} \tag{6}$$

Parametric values (alongside 95% $\mathcal{CI}$):

$p_1 = 0.0003(-0.004, 0.004)$, $p_2 = 0.5(0.2, 1)$, $p_3 = -14(-20, -7)$, $q_1 = -14(-14, -12)$.

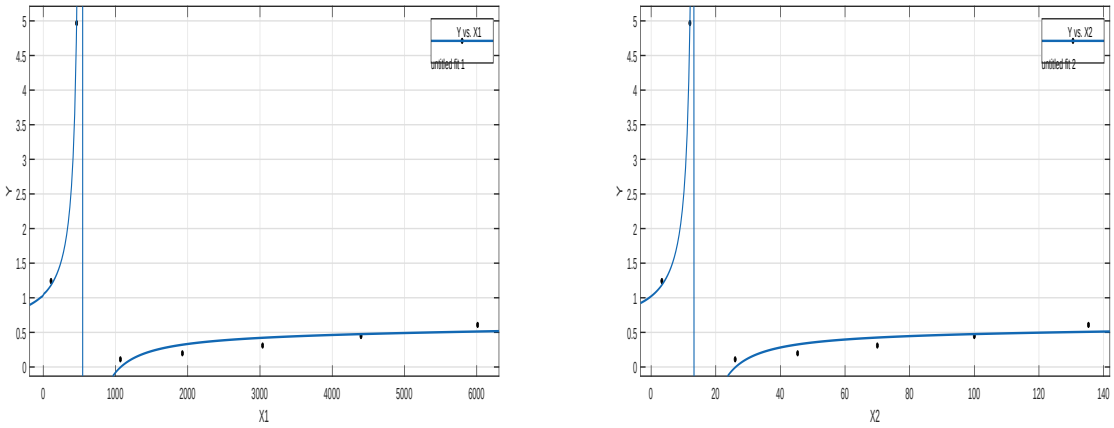

(a) (b)

Figure 49: (a) $\mathcal{R}_1$ vs $\mathcal{HoF}$ (b) $\mathcal{R}_{-1}$ vs $\mathcal{HoF}$

$$\mathcal{HoF}(\mathcal{R}_{\frac{1}{2}}) = \frac{p_1 \times \mathcal{R}_{\frac{1}{2}}^2 + p_2 \times \mathcal{R}_{\frac{1}{2}} + p_3}{\mathcal{R}_{\frac{1}{2}}^2 + q_1 \times \mathcal{R}_{\frac{1}{2}} + q_2} \tag{7}$$

Parametric values (alongside 95% $\mathcal{CI}$):

$p_1 = 0.552(0.3, 0.8)$, $p_2 = 0.5(0.3, 0.8)$, $p_3 = 0.1114(-0.06, 0.3)$, $q_1 = 1.249(0.5, 2)$, $q_2 = 0.3272(-0.3, 1)$.

$$\mathcal{HoF}(\mathcal{R}_{-\frac{1}{2}}) = \frac{p_1 \times (\mathcal{R}_{-\frac{1}{2}})^2 + p_2 \times \mathcal{R}_{-\frac{1}{2}} + p_3}{(\mathcal{R}_{-\frac{1}{2}})^2 + q_1 \times \mathcal{R}_{-\frac{1}{2}} + q_2} \tag{8}$$

Parametric values (alongside 95% $\mathcal{CI}$):

$p_1 = 0.5561(0.3, 0.8)$, $p_2 = 0.5(0.3, 0.8)$, $p_3 = 0.1(-0.1, 0.3)$, $q_1 = 1.251(0.5, 2)$, $q_2 = 0.3292(-0.3, 1)$.

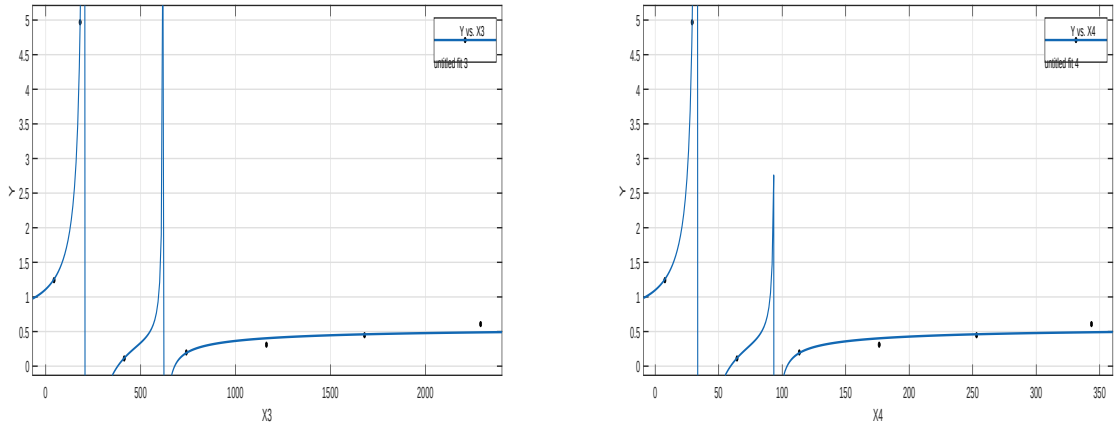

(a) (b)

Figure 50: (a) $\mathcal{R}_{\frac{1}{2}}$ vs $\mathcal{HOF}$ (b) $\mathcal{R}_{-\frac{1}{2}}$ vs $\mathcal{HOF}$

$$\mathcal{HOF}(\mathcal{ABC}) = \frac{p_1 \times (\mathcal{ABC})^2 + p_2 \times (\mathcal{ABC}) + p_3}{\mathcal{ABC} + q_1} \tag{9}$$

Parametric values (alongside 95% $\mathcal{CI}$):

$p_1 = 8e-05(-0.0001, 0.0001)$, $p_2 = 0.5(0.2, 0.9)$, $p_3 = -60(-85, -34)$, $q_1 = -58(-61, -53)$.

$$\mathcal{HOF}(\mathcal{GA}) = \frac{p_1 \times (\mathcal{GA})^2 + p_2 \times (\mathcal{GA}) + p_3}{(\mathcal{GA})^2 + q_1 \times (\mathcal{GA}) + q_2} \tag{10}$$

Parametric values (alongside 95% $\mathcal{CI}$):

$p_1 = 0.5295(0.1, 1)$, $p_2 = -0.4(-2.3, 1.5)$, $p_3 = -0.5(-1.4, 0.5)$, $q_1 = -0.6(-3.8, 2.7)$, $q_2 = -1.281(-4, 1.5)$.

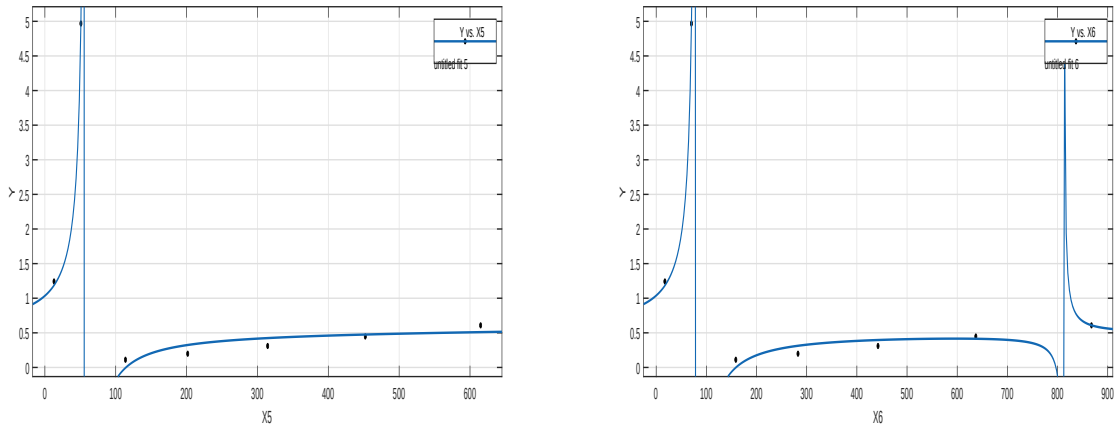

(a) (b)

Figure 51: (a) $\mathcal{AB}$ vs $\mathcal{HOF}$ (b) $\mathcal{GA}$ vs $\mathcal{HOF}$

$$\mathcal{H}o\mathcal{F}(\mathcal{M}_1) = \frac{p_1 \times (\mathcal{M}_1)^2 + p_2 \times (\mathcal{M}_1) + p_3}{\mathcal{M}_1 + q_1} \tag{11}$$

Parametric values (alongside 95% $\mathcal{CI}$):

$p_1 = 1e{-}05(-0.00001, 0.00001)$, $p_2 = 0.5(0.2, 0.9)$, $p_3 = -437(-622, -252)$, $q_1 = -420(-447, -393)$.

$$\mathcal{H}o\mathcal{F}(\mathcal{M}_2) = \frac{p_1 \times (\mathcal{M}_2)^2 + p_2 \times (\mathcal{M}_2) + p_3}{(\mathcal{M}_2)^2 + q_1 \times \mathcal{M}_2 + q_2} \tag{12}$$

Parametric values (alongside 95% $\mathcal{CI}$):

$p_1 = 0.5(0.3, 0.8)$, $p_2 = 0.5(0.3, 0.8)$, $p_3 = 0.1(-0.1, 0.3)$, $q_1 = 1(0.5, 2)$, $q_2 = 0.3(-0.3, 1)$.

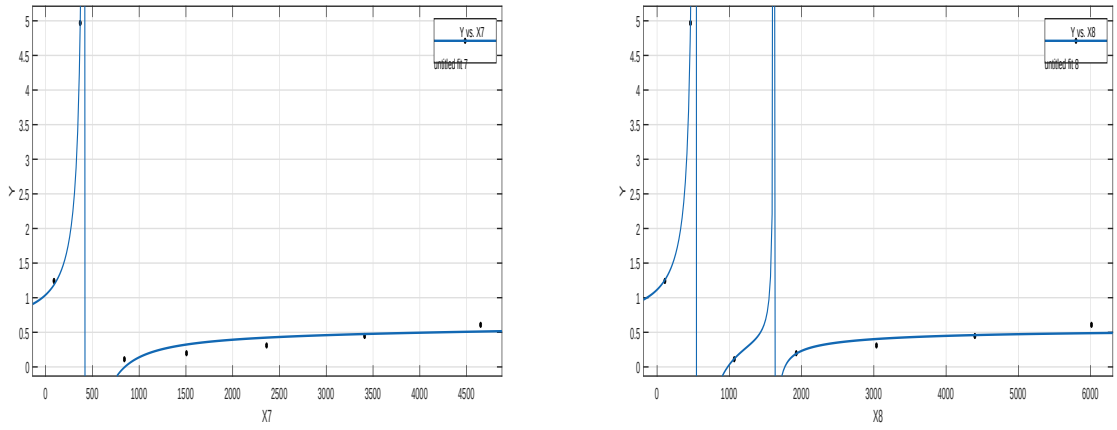

(a) (b)

Figure 52: (a) $\mathcal{M}_1$ vs $\mathcal{H}o\mathcal{F}$ (b) $\mathcal{M}_2$ vs $\mathcal{H}o\mathcal{F}$

$$\mathcal{H}o\mathcal{F}(\overline{\mathcal{M}_1}) = \frac{p_1 \times (\overline{\mathcal{M}_1}) + p_2}{(\overline{\mathcal{M}_1})^4 + q_1 \times (\overline{\mathcal{M}_1})^3 + q_2 \times (\overline{\mathcal{M}_1})^2 + q_3 \times (\overline{\mathcal{M}_1}) + q_4} \tag{13}$$

Parametric values (alongside 95% $\mathcal{CI}$):

$p_1 = 0.01(-2.5, 2.5)$, $p_2 = 0.01(-1.72, 1.74)$, $q_1 = -0.4(-2, 1.22)$, $q_2 = -2.32(-3.7, -1)$, $q_3 = -1.1(-9.196, 7.01)$, $q_4 = -0.02(-5.6, 5.54)$.

$$\mathcal{H}o\mathcal{F}(\overline{\mathcal{M}_2}) = \frac{p_1 \times (\overline{\mathcal{M}_2}) + p_2}{(\overline{\mathcal{M}_2})^2 + q_1 \times (\overline{\mathcal{M}_2}) + q_2} \tag{14}$$

Parametric values (alongside 95% $\mathcal{CI}$):

$p_1 = 3785(-4e+07, 4e+07)$, $p_2 = 2782(-3e+07, 3e+07)$, $q_1 = 1e+04(-1e+08, 1e+08)$, $q_2 = 8467(-9e+07, 9e+07)$.

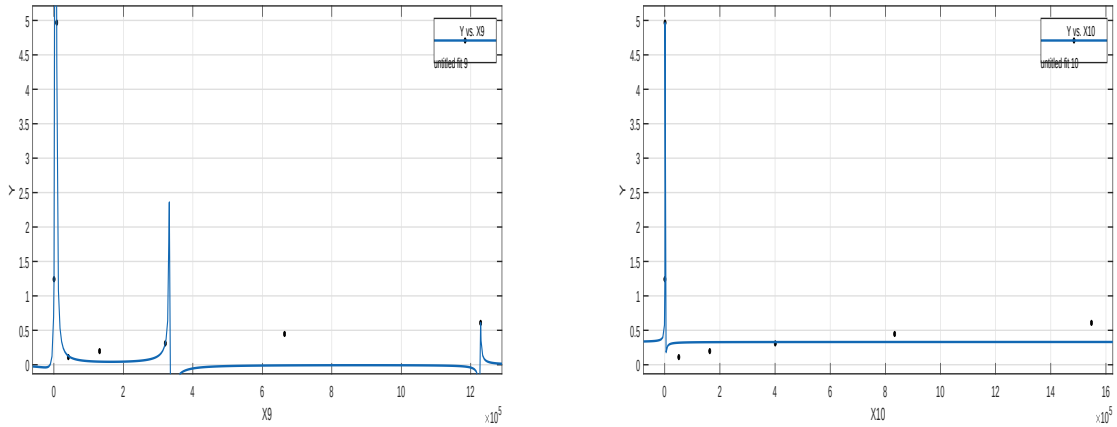

(a) (b)

Figure 53: (a) $\overline{\mathcal{M}_1}$ vs $\mathcal{H}o\mathcal{F}$ (b) $\overline{\mathcal{M}_2}$ vs $\mathcal{H}o\mathcal{F}$

Table 18: Goodness of Fit for $\mathcal{H}o\mathcal{F}$ vs Indices for $g - C_3N_4$.

Index	Fit Type	$\mathcal{SSE}$	$\mathcal{R}^2$	$\mathcal{RMSE}$
$\mathcal{R}_1(\mathcal{G})$	rat32	0.055	0.997	0.234
$\mathcal{R}_{-1}(\mathcal{G})$	rat21	0.058	0.997	0.139
$\mathcal{R}_{\frac{1}{2}}(\mathcal{G})$	rat22	0.023	0.999	0.108
$\mathcal{R}_{-\frac{1}{2}}(\mathcal{G})$	rat22	0.023	0.999	0.107
$\mathcal{ABC}(\mathcal{G})$	rat21	0.056	0.997	0.137
$\mathcal{GA}(\mathcal{G})$	rat22	0.038	0.998	0.138
$\mathcal{M}_1(\mathcal{G})$	rat21	0.056	0.997	0.136
$\mathcal{M}_2(\mathcal{G})$	rat22	0.024	0.999	0.109
$\overline{\mathcal{M}_1}(\mathcal{G})$	rat14	0.232	0.987	0.482
$\overline{\mathcal{M}_2}(\mathcal{G})$	rat12	0.152	0.992	0.225

3.2.5 General models for Indices vs Entropy

Graphical models of entropy vs indices are depicted in figures 54-61.

$$Entropy(\mathcal{R}_1) = \frac{p_1 \times \mathcal{R}_1 + p_2}{\mathcal{R}_1^3 + q_1 \times \mathcal{R}_1^2 + q_2 \times \mathcal{R}_1 + q_3} \tag{15}$$

Coefficients (with 95% confidence bounds):

$p_1 = 0.002(-0.04, 0.04)$, $p_2 = 0.01(-0.03, 0.049)$, $q_1 = 1.9(1.8, 1.93)$, $q_2 = 0.98(0.91, 1.05)$, $q_3 =$

$0.2(0.1, 0.2)$.

$$Entropy(\mathcal{R}_{-1}) = \frac{p_1}{\mathcal{R}_{-1}^3 + q_1 \times \mathcal{R}_{-1}^2 + q_2 \times \mathcal{R}_{-1} + q_3} \tag{16}$$

Parametric values (alongside 95% $\mathcal{CI}$):

$p_1 = 0.01(0.07, 0.01)$, $q_1 = 1.8(1.81, 1.9)$, $q_2 = 0.96(0.92, 0.99)$, $q_3 = 0.14(0.14, 0.15)$.

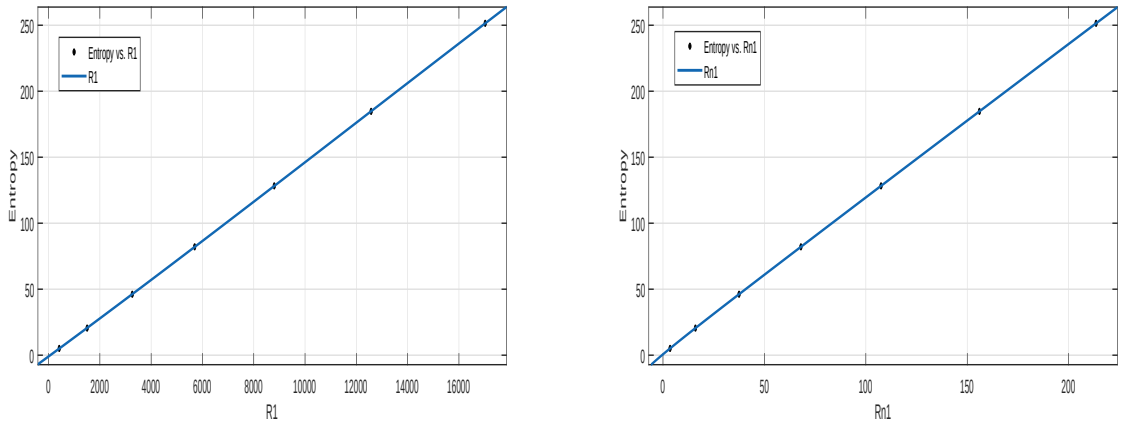

(a) (b)

Figure 54: (a) $\mathcal{R}_1$ vs Entropy (b) $\mathcal{R}_{-1}$ vs Entropy

$$Entropy(\mathcal{R}_{\frac{1}{2}}) = \frac{p_1}{\mathcal{R}_{\frac{1}{2}}^4 + q_1 \times \mathcal{R}_{\frac{1}{2}}^3 + q_2 \times \mathcal{R}_{\frac{1}{2}}^2 + q_3 \times \mathcal{R}_{\frac{1}{2}} + q_4} \tag{17}$$

Parametric values (alongside 95% $\mathcal{CI}$):

$p_1 = 300(-2e+07, 2e+07)$, $q_1 = 9612(-7e+08, 7e+08)$, $q_2 = 1e+04(-1e+09, 1e+09)$, $q_3 = 4311(-3e+08, 3e+08)$, $q_4 = 751(-6e+07, 6e+07)$.

$$Entropy(\mathcal{R}_{-\frac{1}{2}}) = \frac{p_1 \times (\mathcal{R}_{-\frac{1}{2}}) + p_2}{(\mathcal{R}_{-\frac{1}{2}})^3 + q_1 \times (\mathcal{R}_{-\frac{1}{2}})^2 + q_2 \times (\mathcal{R}_{-\frac{1}{2}}) + q_3} \tag{18}$$

Coefficients (with 95% confidence bounds):

$p_1 = 0.001(-0.04, 0.04)$, $p_2 = 0.01(-0.03, 0.05)$, $q_1 = 1.85(1.77, 1.9)$, $q_2 = 0.96(0.9, 1.03)$, $q_3 = 0.15(0.1, 0.18)$.

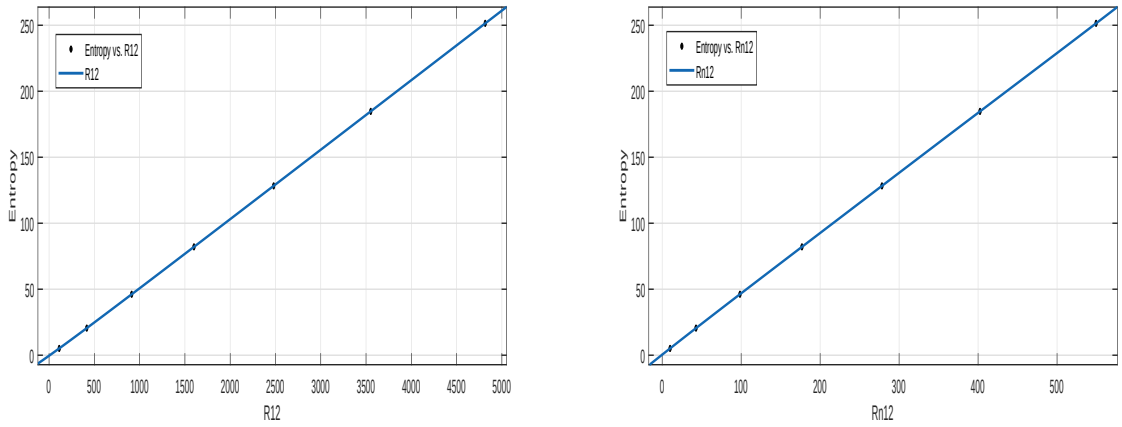

(a) (b)

Figure 55: (a) $\mathcal{R}_{\frac{1}{2}}$ vs *Entropy* (b) $\mathcal{R}_{-\frac{1}{2}}$ vs *Entropy*

$$Entropy(\mathcal{ABC}) = \frac{p_1 \times (\mathcal{ABC})^2 + p_2 \times (\mathcal{ABC}) + p_3}{(ABC)^3 + q_1 \times (\mathcal{ABC})^2 + q_2 \times (\mathcal{ABC}) + q_3} \tag{19}$$

Parametric values (alongside 95% $\mathcal{CI}$):

$p_1 = 3462(-1e+09, 1e+09)$, $p_2 = 2175(-6e+08, 6e+08)$, $p_3 = -1638(-4e+08, 4e+08)$, $q_1 = 2e+04(-6e+09, 6e+09)$, $q_2 = 24e+04(-7e+09, 7e+09)$, $q_3 = 2359(-6e+08, 6e+08)$.

$$Entropy(\mathcal{GA}) = \frac{p_1 \times (\mathcal{GA})^3 + p_2 \times (\mathcal{GA})^2 + p_3 \times (\mathcal{GA}) + p_4}{(\mathcal{GA})^2 + q_1 \times (\mathcal{GA}) + q_2} \tag{20}$$

Parametric values (alongside 95% $\mathcal{CI}$):

$p_1 = -0.001(-0.003, 0.002)$, $p_2 = 0.68(-1.573, 2.931)$, $p_3 = -225(-938.4, 488.6)$, $p_4 = 9956(-3e+04, 5e+04)$, $q_1 = -354(-538.2, -169.2)$, $q_2 = 7061(-1995, 1e+04)$.

$$Entropy(\mathcal{M}_1) = \frac{p_1}{(\mathcal{M}_1)^4 + q_1 \times (\mathcal{M}_1)^3 + q_2 \times (\mathcal{M}_1)^2 + q_3 \times (\mathcal{M}_1) + q_4} \tag{21}$$

Parametric values (alongside 95% $\mathcal{CI}$):

$p_1 = 457(-6e+07, 6e+07)$, $q_1 = 1e+04(-1e+09, 1e+09)$, $q_2 = 1e+04(-2e+09, 2e+09)$, $q_3 = 4538(-6e+08, 6e+08)$, $q_4 = 815(-1e+08, 1e+08)$.

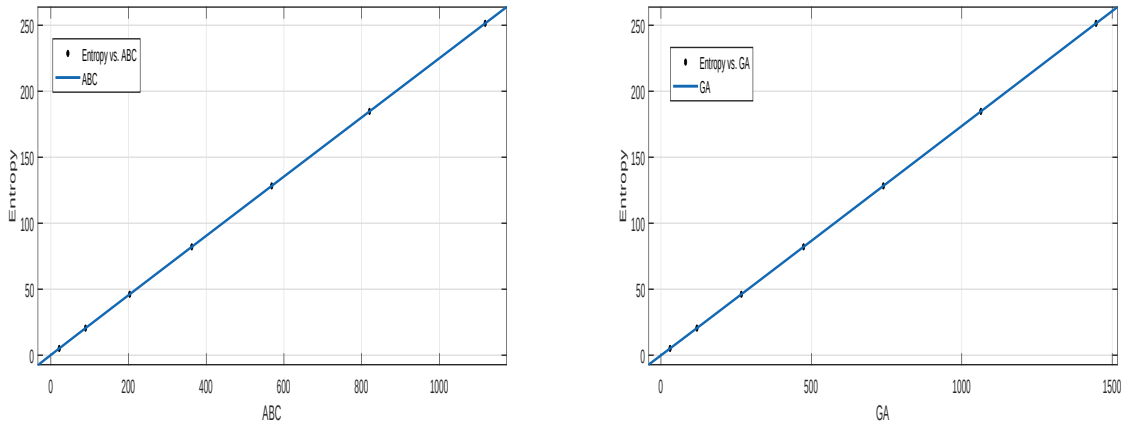

(a) (b)

Figure 56: (a) $\mathcal{AB}$ vs *Entropy* (b) $\mathcal{GA}$ vs *Entropy*

$$Entropy(\mathcal{M}_2) = \frac{p_1}{(\mathcal{M}_2)^4 + q_1 \times (\mathcal{M}_2)^3 + q_2 \times (\mathcal{M}_2)^2 + q_3 \times (\mathcal{M}_2) + q_4} \tag{22}$$

Parametric values (alongside 95% $\mathcal{CI}$):

$p_1 = 461.6(-7e{+}07, 7e{+}07)$, $q_1 = 1e{+}04(-2e{+}09, 2e{+}09)$, $q_2 = 1e{+}04(-2e{+}09, 2e{+}09)$, $q_3 = 3620(-6e+08, 6e+08)$, $q_4 = 673(-1e+08, 1e+08)$.

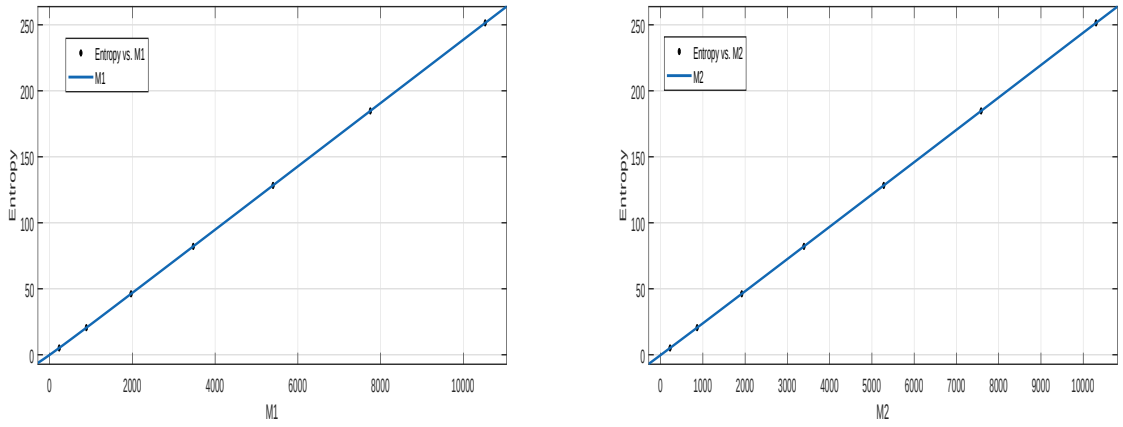

(a) (b)

Figure 57: (a) $\mathcal{M}_1$ vs *Entropy* (b) $\mathcal{M}_2$ vs *Entropy*

$$Entropy(\overline{\mathcal{M}_1}) = \frac{p_1 \times (\overline{\mathcal{M}_1}) + p_2}{(\overline{\mathcal{M}_1})^3 + q_1 \times (\overline{\mathcal{M}_1})^2 + q_2 \times (\overline{\mathcal{M}_1}) + q_3} \tag{23}$$

Parametric values (alongside 95% $\mathcal{CI}$):

$p_1 = 0.003785(-0.0181, 0.02567)$, $p_2 = 0.002874(-0.01328, 0.01903)$, $q_1 = 1.844(1.757, 1.931)$, $q_2 = 1.118(1.038, 1.197)$, $q_3 = 0.2226(0.2115, 0.2337)$.

$$Entropy(\overline{\mathcal{M}_2}) = \frac{p_1 \times Entropy(\overline{\mathcal{M}_2}) + p_2}{(\overline{\mathcal{M}_2})^3 + q_1 \times (\overline{\mathcal{M}_2})^2 + q_2 \times (\overline{\mathcal{M}_2}) + q_3} \tag{24}$$

Parametric values (alongside 95% $\mathcal{CI}$):

$p_1 = 0.003801(-0.01753, 0.02514)$, $p_2 = 0.002822(-0.01299, 0.01864)$, $q_1 = 1.836(1.732, 1.94)$, $q_2 = 1.108(1.01, 1.207)$, $q_3 = 0.2199(0.2037, 0.2362)$.

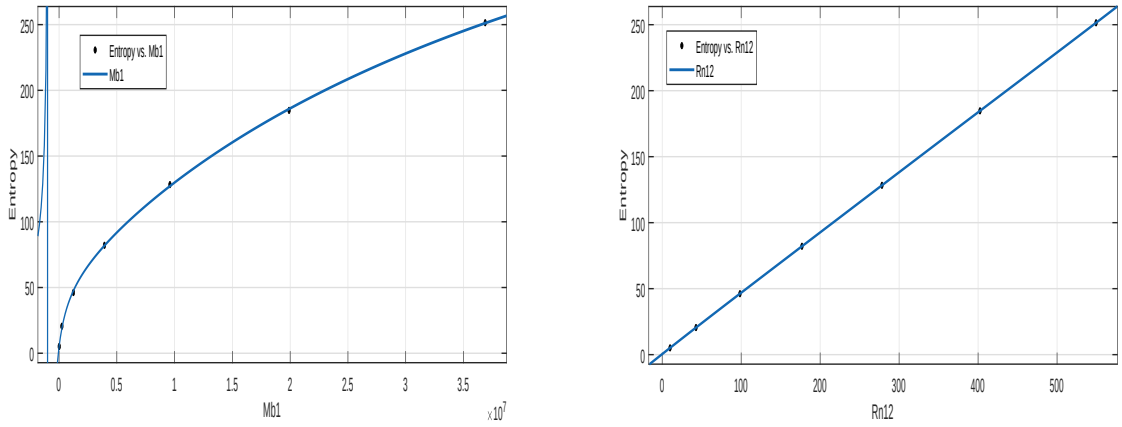

(a) (b)

Figure 58: (a) $\mathcal{R}_{\frac{1}{2}}$ vs *Entropy* (b) $\mathcal{R}_{-\frac{1}{2}}$ vs *Entropy*

$$Entropy(\mathcal{ABC}) = \frac{p_1 \times (\mathcal{ABC})^2 + p_2 \times (\mathcal{ABC}) + p_3}{(\mathcal{ABC})^3 + q_1 \times (\mathcal{ABC})^2 + q_2 \times (\mathcal{ABC}) + q_3} \tag{25}$$

Parametric values (alongside 95% $\mathcal{CI}$):

$p_1 = 3462(-1e+09, 1e+09)$, $p_2 = 2175(-6e+08, 6e+08)$, $p_3 = -1628(-4e+08, 4e+08)$, $q_1 = 2e+04(-6e+09, 6e+09)$, $q_2 = 2e+04(-7e+09, 7e+09)$, $q_3 = 2359(-6e+08, 6e+08)$.

$$Entropy(\mathcal{GA}) = \frac{p_1 \times (\mathcal{GA})^3 + p_2 \times (\mathcal{GA})^2 + p_3 \times (\mathcal{GA}) + p_4}{(\mathcal{GA})^2 + q_1 \times (\mathcal{GA}) + q_2} \tag{26}$$

Parametric values (alongside 95% $\mathcal{CI}$):

$p_1 = -0.0005(-0.003, 0.002)$, $p_2 = 0.68(-1.6, 2.9)$, $p_3 = -225(-938, 489)$, $p_4 = 9956(-3e+04, 5e+04)$, $q_1 = -354(-538, -169.2)$, $q_2 = 7061(-1995, 1e+04)$.

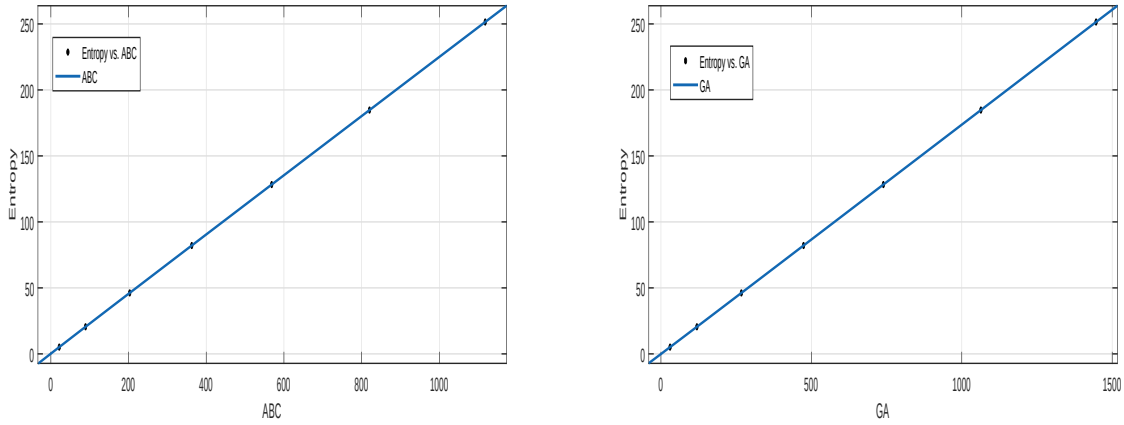

(a) (b)

Figure 59: (a) $\mathcal{AB}$ vs *Entropy* (b) $\mathcal{GA}$ vs *Entropy*

$$Entropy(\mathcal{M}_1) = \frac{p_1}{(\mathcal{M}_1)^4 + q_1 \times (\mathcal{M}_1)^3 + q_2 \times (\mathcal{M}_1)^2 + q_3 \times (\mathcal{M}_1) + q_4} \tag{27}$$

Parametric values (alongside 95% $\mathcal{CI}$):

$p_1 = 458(-1e+07, 6e+07)$, $q_1 = 1e+04(-1e+09, 1e+09)$, $q_2 = 1e+04(-2e+09, 2e+09)$, $q_3 = 4528(-6e+08, 6e+08)$, $q_4 = 816(-1e+08, 1e+08)$.

$$Entropy(\mathcal{M}_2) = \frac{p_1}{(\mathcal{M}_2)^4 + q_1 \times (\mathcal{M}_2)^3 + q_2 \times (\mathcal{M}_2)^2 + q_3 \times (\mathcal{M}_2) + q_4} \tag{28}$$

Parametric values (alongside 95% $\mathcal{CI}$):

$p_1 = 463.6(-8e+07, 8e+07)$, $q_1 = 1e+04(-2e+09, 2e+09)$, $q_2 = 1e+04(-3e+09, 3e+09)$, $q_3 = 3720(-6e+08, 6e+08)$, $q_4 = 663(-1e+08, 1e+08)$.

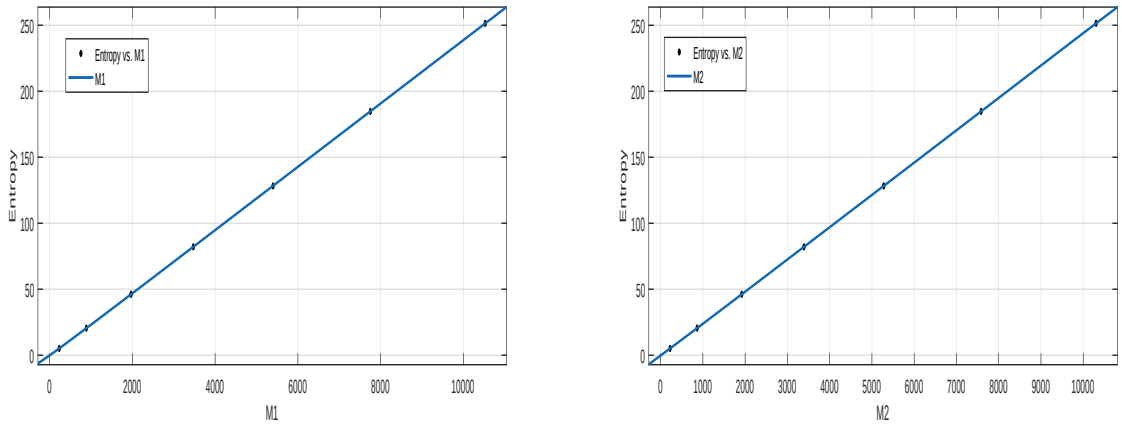

(a) (b)

Figure 60: (a) $\mathcal{M}_1$ vs *Entropy* (b) $\mathcal{M}_2$ vs *Entropy*

$$Entropy(\overline{\mathcal{M}_1}) = \frac{p_1 \times (\overline{\mathcal{M}_1}) + p_2}{(\overline{\mathcal{M}_1})^3 + q_1 \times (\overline{\mathcal{M}_1})^2 + q_2 \times (\overline{M_1}) + q_3} \tag{29}$$

Parametric values (alongside 95% $\mathcal{CI}$):

$p_1 = 0.003785(-0.0181, 0.02567)$, $p_2 = 0.002874(-0.01328, 0.01903)$, $q_1 = 1.844(1.757, 1.931)$, $q_2 = 1.118(1.038, 1.197)$, $q_3 = 0.2226(0.2115, 0.2337)$.

$$Entropy(\overline{\mathcal{M}_2}) = \frac{p_1 \times Entropy(\overline{\mathcal{M}_2}) + p_2}{(\overline{\mathcal{M}_2})^3 + q_1 \times (\overline{\mathcal{M}_2})^2 + q_2 \times (\overline{M_2}) + q_3} \tag{30}$$

Parametric values (alongside 95% $\mathcal{CI}$):

$p_1 = 0.003801(-0.01753, 0.02514)$, $p_2 = 0.002822(-0.01299, 0.01864)$, $q_1 = 1.836(1.732, 1.94)$, $q_2 = 1.108(1.01, 1.207)$, $q_3 = 0.2199(0.2037, 0.2362)$.

Table 19: Goodness of Fit for *Entropy* vs Indices for $g - C_3N_4$.

Index	Fit Type	$\mathcal{SSE}$	$\mathcal{R}^2$	$\mathcal{RMSE}$
$\mathcal{R}_1(\mathcal{G})$	rat13	8e-04	1.000	0.020
$\mathcal{R}_{-1}(\mathcal{G})$	rat03	8e-04	1.000	0.017
$\mathcal{R}_{\frac{1}{2}}(\mathcal{G})$	rat04	5e-02	0.998	0.158
$\mathcal{R}_{-\frac{1}{2}}(\mathcal{G})$	rat13	8e-04	1.000	0.020
$\mathcal{ABC}(\mathcal{G})$	rat23	4e-02	0.998	0.197
$\mathcal{GA}(\mathcal{G})$	rat32	4e-03	1.000	0.060
$\mathcal{M}_1(\mathcal{G})$	rat04	6e-02	0.997	0.174
$\mathcal{M}_2(\mathcal{G})$	rat04	7e-02	0.997	0.186
$\overline{\mathcal{M}_1}(\mathcal{G})$	rat13	8e-04	1.000	0.021
$\overline{\mathcal{M}_2}(\mathcal{G})$	rat13	8e-04	1.000	0.021

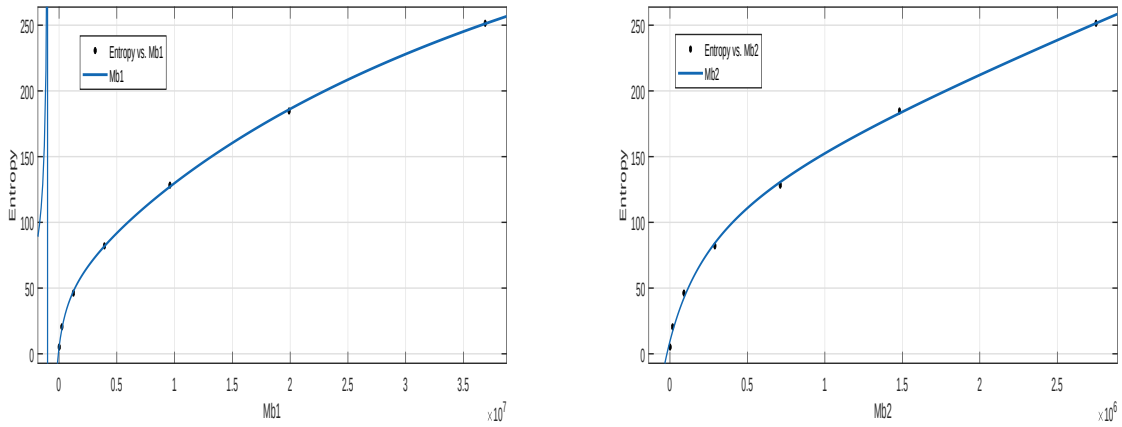

(a) (b)

Figure 61: (a) $\overline{\mathcal{M}_1}$ vs *Entropy* (b) $\overline{\mathcal{M}_2}$ vs *Entropy*

Tables 18 and 19 provide the statistical values for the method of rational fit which provided the least error in case of every fit between indices and HoF and entropy.

Chapter 4

Conclusion

The links between terbium dioxide and thermodynamical characteristics have been developed based on mathematical models. Graphical illustrations have also been provided. This research aids in a deeper understanding of the chemical structure of terbium dioxide based on the graphical qualities of its corresponding chemical graph which is more cost-effective and efficient. The relationships between indices & heat of formation and indices & entropy has been shown using curve fitting techniques. The rational fitting strategy was chosen due to its effectiveness. The same methodology was applied on graphite carbon nitride as well.

Chapter 5

References

Bibliography

[1] Abanades, S. (2019). Metal oxides applied to thermochemical water-splitting for hydrogen production using concentrated solar energy. ChemEngineering, 3(3), 63.

[2] Alizadeh, T., Nayeri, S., & Hamidi, N. (2019). Graphitic carbon nitride ($gC3N4$) graphite nanocomposite as an extraordinarily sensitive sensor for sub-micromolar detection of oxalic acid in biological samples. RSC advances, 9(23), 13096-13103.

[3] Ami, D., Belo, D., Luci, B., Nikoli, S., & Trinajsti, N. (1998). The vertex-connectivity index revisited. Journal of chemical information and computer sciences, 38(5), 819-822.

[4] Balabanov, S. S., et al., Synthesis and structural characterization of ultrafine terbium oxide powders. Ceramics International, 2017. 43(18), 16569-16574.

[5] Balaban. A. T. (1982). Highly discriminating distance-based topological index, Chemical Physics Letters, vol. 89, no. 5, 399–404.

[6] Balaban, A. T., & Quintas, L. V. (1983). The smallest graphs, trees, and 4-trees with degenerate topological index, Journal of Mathematical Chemistry, vol. 14, pp. 213–233.

[7] Barraclough, K. G., Robbins, D. J., & Canham, L. T. (1991). Silicon electroluminescent device. Google Patents.

[8] Bhosale, R., Kumar, A., AlMomani, F. (2016). Solar thermochemical hydrogen production via terbium oxide based redox reactions. International Journal of Photoenergy, 2016.

[9] Bollobs, B., & Erds, P. (1998). Graphs of extremal weights. Ars Combinatoria, 50, 225-233.

[10] Burroughes, J. H., et al., Light-emitting diodes based on conjugated polymers. nature, 1990. 347(6293), 539-541.

[11] Cao, Q., Kumru, B., Antonietti, M., & Schmidt, B. V. (2020). Graphitic carbon nitride and polymers: a mutual combination for advanced properties. Materials Horizons, 7(3), 762-786.

[12] Gonalves, D. A., Alvim, R. P., Bicalho, H. A., Peres, A. M., Binatti, I., Batista, P. F.,& Lorenson, E. (2018). Highly dispersed Mo-doped graphite carbon nitride: potential application as oxidation catalyst with hydrogen peroxide. New Journal of Chemistry, 42(8), 5720-5727.

[13] Caporossi, G., Gutman, I., Hansen, P., & Pavlovi, L. (2003). Graphs with maximum connectivity index. Computational Biology and Chemistry, 27(1), 85-90.

[14] Doli, T. (2008). Vertex-weighted Wiener polynomials for composite graphs. Ars Mathematica Contemporanea, 1(1), 66-80.

[15] dos Santos, A. M., et al. (2006). Photoluminescence of lanthanide NASICONs: Na 5 LnSi 4 O 12, Ln= Eu, Tb. Journal of Materials Chemistry, 16(30), 3139-3144.

[16] Edwards, A., et al. (1997). Synthesis and characterization of electroluminescent organolanthanide (III) complexes. Synthetic metals, 84(1-3), 433-434.

[17] Estrada, E., Torres, L., Rodriguez, L., & Gutman, I. (1998). An atom-bond connectivity index: modelling the enthalpy of formation of alkanes.

[18] Furtula, B., Graovac, A., Vukičević, D. (2010). Augmented Zagreb index, Journal of Mathematical Chemistry, vol. 48, no. 2, 370–380.

[19] Ghorbani, M., Azimi, N. (2012). Note on multiple Zagreb indices, Iranian Journal of Mathematical Chemistry, vol. 3, no. 2, 137–143.

[20] Gschneidner, K.A., Bunzli, J. C. G., & Pecharsky, V. K. (2004). Handbook on the physics and chemistry of rare earths, Elsevier.

[21] Gutman, I., & Das, K. C. (2004). The first Zagreb index 30 years after. MATCH Commun. Math. Comput. Chem, 50(1), 83-92

[22] Gutman, I., Furtula, B., Vukicevic, Z. K., & Popivoda, G. (2015). On Zagreb indices and coindices. MATCH Commun. Math. Comput. Chem, 74(1), 5-16.

[23] Gutman, I., & Trinajsti, N. (1972). Graph theory and molecular orbitals. Total π-electron energy of alternant hydrocarbons. Chemical Physics Letters, 17(4), 535-538.

[24] Gutman, I., & Trinajsti, N. (1972). Graph theory and molecular orbitals. Total π-electron energy of alternant hydrocarbons. Chemical Physics Letters, 17(4), 535-538.

[25] Liu, H., Wang, X., Wang, H., & Nie, R. (2019). Synthesis and biomedical applications of graphitic carbon nitride quantum dots. Journal of Materials Chemistry B, 7(36), 5432-5448.

[26] Liu, J., Wang, H., & Antonietti, M. (2016). Graphitic carbon nitride reloaded: emerging applications beyond (photo) catalysis. Chemical Society Reviews, 45(8), 2308-2326.

[27] Li, L., et al. (2017). Multicolor light-emitting devices with Tb 2 O 3 on silicon. Scientific Reports, 7(1), 1-4.

[28] Li, X., Gutman, I., & Randi, M. (2006). Mathematical aspects of Randi-type molecular structure descriptors. University, Faculty of Science.

[29] Lyth, S. M., Nabae, Y., Islam, N. M., Kuroki, S., Kakimoto, M. A., Ozaki, J. I., & Miyata, S. (2010). Electrochemical oxygen reduction on carbon nitride. ECS Transactions, 28(23), 11-31.

[30] Oh, J., Yoo, R. J., Kim, S. Y., Lee, Y. J., Kim, D. W., & Park, S. (2015). Oxidized carbon nitrides: waterdispersible, atommically thin carbon nitride based nanodots and their performances as bioimaging probes. ChemistryA European Journal, 21(16), 6241-6246.

[31] Ong, W. J., Tan, L. L., Ng, Y. H., Yong, S. T., & Chai, S. P. (2016). Graphitic carbon nitride (g-C3N4)-based photocatalysts for artificial photosynthesis and environmental remediation: are we a step closer to achieving sustainability?. Chemical reviews, 116(12), 7159-7329.

[32] Randic, M. (1975). Characterization of molecular branching. Journal of the American Chemical Society, 97(23), 6609-6615.

[33] Ranjini, P. S., Lokesha, V., & Usha, A. (2013). "Relation between phenylene and hexagonal squeeze using harmonic index," International Journal of Applied Graph Theory, vol. 1, no. 4, pp. 116–121.

[34] Singh, S., et al. (2013). Fabrication of nanobeads structured perovskite type neodymium iron oxide film: its structural, optical, electrical and LPG sensing investigations. Sensors and Actuators B: Chemical, 177: p. 730-739.

[35] Steckl, A. J., et al. (2002). Rare-earth-doped GaN: growth, properties, and fabrication of electroluminescent devices. IEEE Journal of Selected Topics in Quantum Electronics, 8(4), 749-766.

[36] Su, Q., Sun, J., Wang, J., Yang, Z., Cheng, W., & Zhang, S. (2014). Urea-derived graphitic carbon nitride as an efficient heterogeneous catalyst for CO 2 conversion into cyclic carbonates. Catalysis Science & Technology, 4(6), 1556-1562.

[37] Vukičević, D., Furtula, B. (2009). Topological index based on the ratios of geometrical and arithmetical means of end-vertex degrees of edges. Journal of mathematical chemistry, 46(4), 1369-1376.

[38] Xu, D., Dong, L., & Ren, J. (2017). Introduction of hydrogen routines, in Hydrogen Economy, Elsevier, 35-54.

[39] Ziani, A., et al. (2014). Annealing effects on the photoluminescence of terbium doped zinc oxide films. Thin Solid Films, 553, 52-57.